1. Report No. **FHWA/LA.16/xxx**	2. Government Accession No.	3. Recipient's Catalog No.
4. Title and Subtitle **Design and Investigation of a Fuel-Flexible Injection System for Low-Emission Vehicles**	5. Report Date June 2017	
	6. Performing Organization Code LTRC Project Number: 17-3TIRE SIO Number: DOTLT1000137	
7. Author(s) Lulin Jiang, Ph.D. Oladapo S. Akinyemi, Vu Danh	8. Performing Organization Report No.	
9. Performing Organization Name and Address Department of Mechanical Engineering University of Louisiana at Lafayette Lafayette, LA 70503	10. Work Unit No. 11. Contract or Grant No.	
12. Sponsoring Agency Name and Address Louisiana Department of Transportation and Development P.O. Box 94245 Baton Rouge, LA 70804-9245	13. Type of Report and Period Covered **[Final Report]** **[July 2016-June 2017]** 14. Sponsoring Agency Code	

15. Supplementary Notes

Conducted in Cooperation with the U.S. Department of Transportation, Federal Highway Administration

16. Abstract

The transportation sector represented 27% of total U.S. greenhouse gas (GHG) emissions, all from fuel combustion, in 2013 according to the U.S. Greenhouse Gas Inventory Report: 1990-2013. The National Science Foundation (NSF) and Department of Energy (DOE) have urged researches on clean and efficient vehicles facing the ever increasing energy demand and aggravating GHG effect. Clean and complete combustion of liquid fuels highly relies on fine sprays evaporating quickly and mixing well with oxidizer and thus, burning cleanly and more completely. However, present fuel injection systems cannot finely atomize and thus cleanly combust viscous fuels. Also, the fluctuating oil price and high cost of biofuels obstructs the widespread utilization of renewable fuels. Recently, a novel flow-blurring (FB) injector has been developed by PI and collaborators and proved to generate fine sprays, instead of typical jets, immediately at the injector exit and result in ultra-low-emission combustion of fuels including conventional diesel and biodiesel and its source oil - vegetable oil (VO) as well as its waste byproduct - straight glycerol (about 200 times more viscous than diesel), without fuel-preheating and hardware modification. However, the detailed atomization mechanism is yet unknown limiting its practical application. Also for highly viscous glycerol, previous spray imaging has shown droplets and ligaments are generated at injector exit, resulting in extended pre-vaporization zone and lifted glycerol flame, that is easier to be blown off, and causing relatively higher emissions.

The present research seeks to further enhance atomization and stabilize spray and thus combustion, especially for viscous fuels including VO and algae oil (AO). A novel swirl burst (SB) injector is successfully designed in the current work by incorporating a swirling atomizing air with the flow blurring concept. Results show clean lean premixed combustion of viscous and heavy source oils (VO and AO) of biodiesel have been achieved using the novel SB injection without fuel pre-heating. This signifies greatly saving the cost and energy of converting the source oils into biodiesel for conventional engines running on low viscosity fuels. Compared the FB injector, SB injection results in enhanced atomization, and thus faster fuel pre-vaporization, improved fuel-air mixing, hence less lifted flames with ultra-low emissions. Swirl number (SN) of 2.0 is found to give the optimum SB injector geometry with lowest emissions among three teste SNs of 1.5, 2.0 and 2.4. Spray characteristics using Particle Image Velocimetry quantitatively substantiate the further improved atomization of the SB injector. Pressure measurements in the flow line indicates the novel SB injection with high viscosity tolerance requires much lower energy input than the conventional AB injector, showing the promise of developing next-generation clean engines on heavy fuels with higher power-to-weight ratio. Compared to a FB injector, SB injection enhances the spray fineness without extra energy input. Overall, the novel SB injector indicates the promise for clean vehicles such as microturbine-driven hybrid vehicles (cars, trucks, and boats) and airplane powered by jet engines.

17. Key Words	18. Distribution Statement
Swirl Burst Injector, Fuel-Flexible, Vegetable oil, Algae oil, Low Emissions, Lean Premixed (LPM) Combustion, Particle Imaging Velocimetry (PIV)	**Unrestricted. This document is available through the National Technical Information Service, Springfield, VA 21161.**

19. Security Classif. (of this report)	20. Security Classif. (of this page)	21. No. of Pages	22. Price

Project Review Committee

Each research project will have an advisory committee appointed by the LTRC Director. The Project Review Committee is responsible for assisting the LTRC Administrator or Manager in the development of acceptable research problem statements, requests for proposals, review of research proposals, oversight of approved research projects, and implementation of findings.

LTRC appreciates the dedication of the following Project Review Committee Members in guiding this research study to fruition.

LTRC Administrator/Manager

[Enter name]

[Enter field of research] Research Manager

Members

[List all PRC members—one name per line]

Directorate Implementation Sponsor

Janice P. Williams, P.E.

DOTD Chief Engineer

Design and Investigation of a Fuel-Flexible Injection System for Low-Emission Vehicles

by

Lulin Jiang, Ph.D.
Assistant Professor

Oladapo S. Akinyemi
Graduate Student

Vu Danh
Graduate Student

Department of Mechanical Engineering
241 E. Lewis St. Rougeau Hall
University of Louisiana at Lafayette
Lafayette, LA 70503

LTRC Project No. 17-3TIRE
SIO No. DOTLT1000137
conducted for

Louisiana Department of Transportation and Development
Louisiana Transportation Research Center

June 2017

ABSTRACT

The transportation sector represented 27% of total U.S. greenhouse gas (GHG) emissions, all from fuel combustion, in 2013 according to the *U.S. Greenhouse Gas Inventory Report: 1990-2013*. The National Science Foundation (NSF) and Department of Energy (DOE) have urged researches on clean and efficient vehicles facing the ever increasing energy demand and aggravating GHG effect. Clean and complete combustion of liquid fuels highly relies on fine sprays evaporating quickly and mixing well with oxidizer and thus, burning cleanly and more completely. However, present fuel injection systems cannot finely atomize and thus cleanly combust viscous fuels. Also, the fluctuating oil price and high cost of biofuels obstructs the widespread utilization of renewable fuels. Recently, a novel flow-blurring (FB) injector has been developed by PI and collaborators and proved to generate f**ine sprays, instead of typical jets, immediately at the injector exit** and result in ultra-low-emission combustion of fuels including conventional diesel and biodiesel and its source oil - vegetable oil (VO) as well as its waste byproduct - straight **glycerol (about 200 times more viscous than diesel), without fuel-preheating and hardware modification.** However, the detailed atomization mechanism is yet unknown limiting its practical application. Also for highly viscous glycerol, previous spray imaging has shown droplets and ligaments are generated at injector exit, resulting in extended pre-vaporization zone and lifted glycerol flame, that is easier to be blown off, and causing relatively higher emissions.

The present research seeks to further enhance atomization and stabilize spray and thus combustion, especially for viscous fuels including VO and algae oil (AO). A novel swirl burst (SB) injector is successfully designed in the current work by incorporating a swirling atomizing air with the flow blurring concept. Results show clean lean premixed combustion of viscous and heavy source oils (VO and AO) of biodiesel have been achieved using the novel SB injection without fuel pre-heating. This signifies greatly saving the cost and energy of converting the source oils into biodiesel for conventional engines running on low viscosity fuels. Compared the FB injector, SB injection results in enhanced atomization, and thus faster fuel pre-vaporization, improved fuel-air mixing, hence less lifted flames with ultra-low emissions. Swirl number (SN) of 2.0 is found to give the optimum SB injector geometry with lowest emissions among three teste SNs of 1.5, 2.0 and 2.4. Spray characteristics using Particle Image Velocimetry quantitatively substantiate the further improved atomization of the SB injector. Pressure measurements in the flow line indicates the novel SB injection with high viscosity tolerance requires much lower energy input than the conventional AB injector, showing the promise of developing next-generation clean engines on heavy fuels with higher power-to-weight ratio. Compared to a FB injector, SB injection enhances the spray fineness without extra energy input. Overall, the novel SB injector indicates the promise for clean vehicles such as microturbine-driven hybrid vehicles (cars, trucks, and boats) and airplane powered by jet engines.

ACKNOWLEDGMENTS

The PI would like to acknowledge the funding support for this research by the Louisiana Department of Transportation and Development (DOTD) through the Louisiana Transportation Research Center (LTRC). Special thanks to Dr. VJ Gopu for his support of this research. The PI also sincerely thank for Dr. Charles Tayler and Mr. Jeff Guidry at University of Louisiana at Lafayette (UL Lafayette) on the manufacturing of the designed new fuel injector. The PI also gratefully acknowledge the support of her mother institution (UL Lafayette) to establish the combustion and spray experiment facilities and procure the high-spatial resolution Particle Image Velocimetry (PIV) used in the current study. The PI would like to acknowledge the travel grant provided by LTRC to attend the 10th National Combustion Conference to present the results of this study in a technical paper with an oral presentation. The PI highly acknowledges the diligent and productive work of the doctoral student, Mr. Oladapo S Akinyemi on combustion tests, the master student, Mr. Vu Danh on spray PIV investigation, and the undergraduate research assistant John T. Frank on manufacturing the injector with high precision, as well as the assistance of prior undergraduate student Tyler Vining. Thanks to LTRC for agreeing to publish the results of this report.

IMPLEMENTATION STATEMENT

The results obtained from the current project show promises of direct clean and efficient combustion of various heavy and viscous fuels using the designed novel swirl burst (SB) injector without fuel pre-processing. The novel injection enables ultra-low emission combustion of straight algae oil, the third generation of biodiesel source oil, saving the great cost and energy of converting it into low-viscosity biodiesel for existing combustion systems. The novel fuel injection can be used to develop next-generation fuel-flexible engines operating on heavy and viscous oils for low-emission vehicles. The methodology presented in this report is applicable to investigate combustion and spray characteristics of fuel injectors for potential implementation in the practical combustion systems firing on fuel sprays.

TABLE OF CONTENTS

ABSTRACT III

ACKNOWLEDGMENTS V

IMPLEMENTATION STATEMENT VII

TABLE OF CONTENTS IX

LIST OF TABLES XI

LIST OF FIGURES XIII

INTRODUCTION 1

OBJECTIVE 3

SCOPE 4

METHODOLOGY 5

Design of the Novel Swirl Burst Injector 5

Experimental Setup of Combustion Performance of the SB Injector 6

Combustion of Vegetable Oil (VO) using the SB injector 6

Effect of SB Injector Geometry on Combustion of Algae Oil (AO) 8

Spray Characterization using Particle Image Velocimetry (PIV) 9

Experimental Setup of the Spray Injection System 9

Particle image velocimetry (PIV) Setup and Data Processing 10

DISCUSSION OF RESULTS 12

Combustion Performance of the SB injector on Vegetable Oil (VO) 12

Effect of Swirling Atomizing Air 12

Effect of atomizing air to liquid mass ratio (ALR) of the SB Injector 15

Effect of the SB Injector Geometry on Combustion of Algae Oil 18

Comparison of Spray Characteristics of SB and FB injectors 21

CONCLUSIONS 31

RECOMMENDATIONS 33

ACRONYMS, ABBREVIATIONS, AND SYMBOLS 34

REFERENCES 37

APPENDIX 39

LIST OF TABLES

Table 1 Physical and chemical properties of different liquid fuels 6

LIST OF FIGURES

Figure 1 Working principle of a FB injector 1

Figure 2 Schematics of (a) Flow blurring concept and (b) Swirl burst concept 5

Figure 3Schematics of Experiment Setup of the Combustion System using the SB or FB injector 7

Figure 4 Injection system 10

Figure 5 PIV experimental setup 10

Figure 6 Flame images of the combustion of VO at ALR = 3.5 for (a) FB (b) SB injector ... 13

Figure 7 Temperature distribution of combustor outside wall 13

Figure 8 Radial profile of product gas temperature at the combustor exit 13

Figure 9 Radial profile of CO emissions 14

Figure 10 Radial profile of NOx emissions 14

Figure 11 Flame images of the combustion of VO using SB injector at ALRs of (a) 3.0 (b) 3.5 (c) 4.0 15

Figure 12 Temperature distribution of combustor outside wall at various ALRs 15

Figure 13 Radial profile of product gas temperature of SB injector at different ALRs 16

Figure 14 Radial profile of CO emissions of SB injector at different ALRs 17

Figure 15 Radial profile of NOx emissions of SB injector at different ALRs 17

Figure 16 AO Flame images using SB injector at ALR = 4.0 with SN (a) 1.5 (b) 2.0 (c) 2.4 18

Figure 17 Axial profile of combustor outside wall temperature for SB injector with varying swirl number 18

Figure 18 Radial profile of CO emissions for SB injector with varying swirl number 20

Figure 19 Radial profile of NOx emissions for SB injector with varying swirl number 20

Figure 20 Radial profile of product gas temperature for SB injector with varying swirl number 21

Figure 21 Water spray image of (a) FB injector, (b) SB injector at the injector near field with the FOV of 10mm by 10mm 22

Figure 22 Time-averaged field of droplet velocity magnitude contours for (a) FB injector, (b) SB injector 22

Figure 23 Time-average field of droplet axial velocity for (a) FB injector, (b) SB injector .. 23

Figure 24 Time-average field of droplet radial velocity for (a) FB injector, (b) SB injector . 24

Figure 25 Droplet axial velocity profile of time-average for (a) FB injector, (b) SB injector 25

Figure 26 Droplet radial velocity profile of time-average for (a) FB injector, (b) SB injector 25

Figure 27 Time analysis of droplet axial velocity at x = 0mm for (a) – (d) FB injector, (e) – (h) SB injector. 27

Figure 28 Time analysis of droplet axial velocity at x = 1 mm for (a) – (d) FB injector, (e) – (h) SB injector. 28

Figure 29 Probability distribution plots of droplet radial velocity at the center spray at different axial locations for: (a) FB injector, (b) SB injector 29

Figure 30 Pressure drop of atomizing air line across injectors 30

INTRODUCTION

Dramatic increases in energy utilization and aggravating global warming imperatively desire a stricter emission standard and thus require efficient and clean fuel consumption. The transportation sector represented 27% of total U.S. greenhouse gas (GHG) emissions in 2013 according to the *U.S. Greenhouse Gas Inventory Report: 1990-2013*. These transportation emissions are all via fuel combustion of all vehicles for sea, space and land use. In order to satisfy stricter emission standards and increasing energy demand, it is imperative to consume fuels more efficiently and cleanly, and explore renewable energy resources for transportation means. Correspondingly, National Science Foundation (NSF) and Department of Energy (DOE) have urged research on clean hybrid vehicles and aero jet engines with improved fuel efficiency, clean fuel consumption including fossil fuels and biofuels.

Biodiesel is the most common alternative drop-in vehicle fuel because of its similar property to diesel, the closed-carbon cycle and thus low greenhouse gas (GHG) effect. However, the widespread application of biodiesel is limited mainly due to (1) high production cost by converting viscous vegetable oils (VO), algae oil (AO) or other feedstock, (2) cost for coping with highly viscous waste byproduct - glycerol. Clean and complete combustion of liquid fuels highly relies on spray fineness leading to faster fuel evaporation, well mixed fuel-air mixture and the subsequent clean premixed combustion. Application of other bio-oils is yet impractical mainly because of the high viscosity and limitation of present fuel injection systems that cannot finely atomize and cleanly combust viscous fuels. For continuous flow applications, conventional air-blast (AB) injectors generate liquid fuel jet first which disintegrates into droplets at further downstream for fuels with low viscosities.

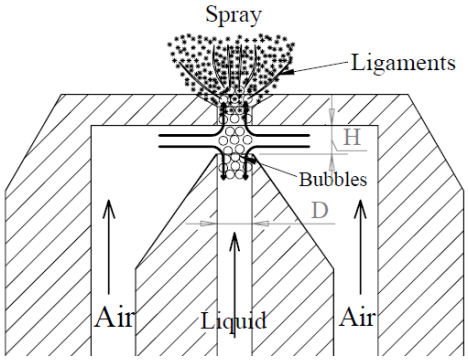

Figure 1
Working principle of a FB injector

Fortunately, Gañán-Calvo (2005) reported a novel flow blurring (FB) injection concept which produces finer droplets with up to fifty times surface area to volume ratio and atomization efficiency ten times compared to AB atomization *[1]*. In FB atomization, the atomizing air passes through a gap between the exit of the liquid tube and the concentric injector orifice at a distance H downstream of the liquid tube, see Figure 1. FB is reported to be effective when the diameter D of internal liquid tube

and injector orifice are identical, and H ≤ 0.25D *[1]*. The atomizing air flow bifurcates at a stagnation point created between the liquid tube and orifice exit. A portion of the bifurcated air stream penetrates into the liquid tube forming a two-phase flow near the liquid tube exit while the other portion flows out through the orifice. The two-phase mixture (liquid and bubbles) experiences a sudden pressure drop while exiting the injector. Thus, bubbles expand and bursts, deforming the surrounding liquid into fine spray immediately at the injector exit, rather than typical liquid jet of a conventional AB atomizer.

The supreme FB atomization has resulted in clean combustion of different fuels with widely varied viscosities *[2-6]*. These fuels include kerosene, diesel, biodiesel, and even viscous straight VO and glycerol without fuel-preheating, signifying that the cost of biofuel production can be significantly reduced without converting the source oils such as VO and/or post-processing glycerol. Thus, FB injection potentially enables widespread use of biofuel and development of combustion systems with high fuel-flexibility. The fineness of FB sprays allowed optical accessibility in the injector near field. Jiang and Agrawal (2015) investigated the FB atomization in the nozzle near region for water and highly viscous glycerol using spatially-resolved high-speed imaging and Particle Image Velocimetry (PIV) *[7, 8]*. They found that most of water has been atomized into droplets at the nozzle exit with relatively larger ones at the spray periphery because of the bubble bursting, characterized as the primary FB breakup *[7]*. Interestingly, for viscous glycerol, both fine droplets and thin ligaments were observed from the primary atomization *[8]*. The larger droplets and ligaments underwent secondary breakup by Rayleigh-Taylor's instabilities between the liquid phase and high-velocity atomizing air *[7, 8]*. For viscous liquids such as glycerol, the secondary atomization is more significant, representative of longer secondary atomization length of about 30 mm downstream the injector exit, while around 4 mm was investigated to complete the water atomization for a FB injector with D = 1.5 mm *[7, 8]*. As a result, compared to other fuels, longer fuel pre-vaporization and fuel-air mixing region was needed for clean premixed combustion of glycerol, leading to more lifted-up flames which might offset the flame stabilities and sustainability *[2-6]*.

The present study aims to further improve the secondary atomization of viscous liquids with smaller droplets, leading to faster vaporization, better fuel-air mixing and hence less emissions.

OBJECTIVE

The ultimate goal of this work is to establish a successful research program in efficient and clean combustion area that will tackle the environmental and economic barriers of burning both fossil and alternative fuels, and cope with the fluctuating oil price with system fuel flexibility. The overall objective of this study is to develop a fuel-flexible injection system with enhanced atomization capability for low-emission vehicles without fuel-preheating or hardware modification. The system can be employed in any continuous spray applications including microturbine-powered hybrid vehicles (cars, trucks, and boats) and airplane jet engines.

Specifically, the main objectives of the present research are:

- to design a swirl burst (SB) injector to enhance atomization of viscous fuels in the injector near region by designing swirling air paths and introducing enhanced aerodynamic interaction;
- to estimate fuel flexibility of the SB injector integrating swirl and FB effects by investigating emissions and flame temperatures for various fuels;
- to investigate spray fineness and atomization process;
- to characterize microbial algae oil from combustion perspective and explore the feasibility of direct combustion of algae oil without converting it into biodiesel with high energy input and cost;
- to better understand and exploit the aerodynamics, atomization and combustion response of various injector geometry.

SCOPE

The scope of this work is to design a novel fuel injector for continuous-flow combustion systems which can be used for hybrid low-emission vehicles. The present work investigates the combustion performance of the novel injector characteristics in terms of flame structure and emissions for various viscous oils in a lab-scale open-end burner. The project also explores the spray characteristics using PIV laser diagnostics system. This work does not pertain to engine assembly or practical engine test.

METHODOLOGY

The present study aims to further improve the secondary atomization of viscous liquids with smaller droplets, leading to faster vaporization, better fuel-air mixing and hence less emissions. A swirl path for atomizing air will be integrated with FB concept. The main effects of swirl are to speed up fuel-air mixing, improve flame stability, and reduce flame length *[9]*. Huang and Yang (2005) found that the swirl intensity had enormous effect on the flow development and flame dynamics in a lean premixed swirl-stabilized combustor *[10]*. These advantages of swirling flow are expected to improve secondary atomization and local fuel-air mixing for stable flames of viscous fuels. Combustion tests, spray investigation as well as data analysis using related technical software will reveal the effectiveness of the new design. The details of methodology are discussed below.

Design of the Novel Swirl Burst Injector

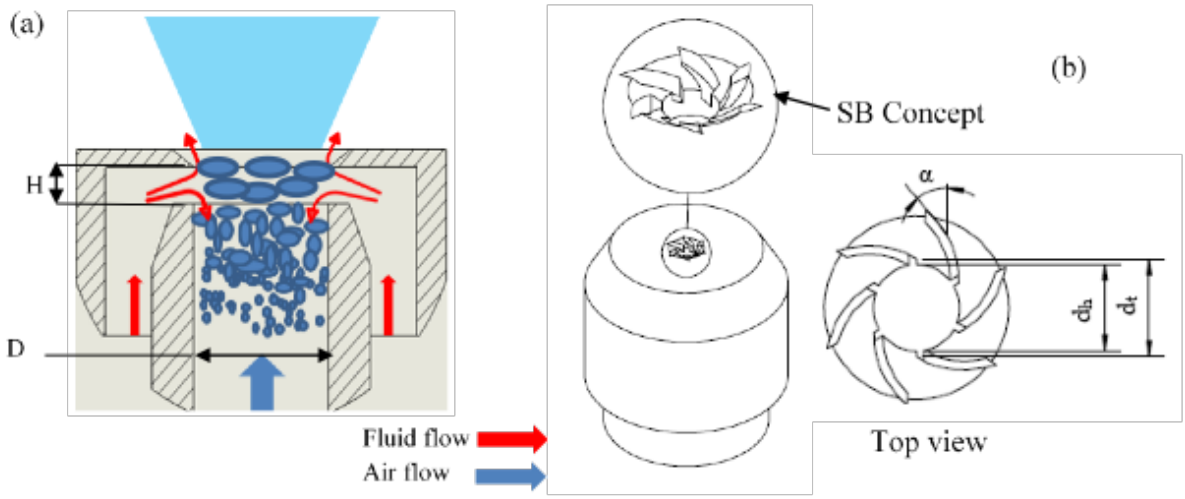

Figure 2
Schematics of (a) Flow blurring concept and (b) Swirl burst concept

The present study designs a new internally mixing twin-fluid injector, called Swirl Burst (SB) injector by incorporating swirling atomizing air and the FB concept to enhance secondary atomization of viscous liquid fuels. In the FB concept, given in Figure 2(a), portion of the bifurcated atomizing air flows back into the internal liquid tube to form a two-phase flow leading to primary atomization. The other portion leaves the injector orifice assisting with the secondary disintegration of larger droplets at spray edge and ligaments of viscous liquids *[7, 8]*. This study incorporates a swirling flow path onto the injector orifice exit route of the FB injector, hence SB injector, for the atomizing air leaving the orifice to

dynamically improve the shear layer interaction between the high-speed swirling air and the droplets and/or ligaments from the primary bubble bursting of viscous liquid fuels. Figure 2(b) shows the design of the novel SB injector with a swirl number of 2.4 used in this study for the SB concept. The swirl number (SN) characterizes the degree of swirl, it is a non-dimensional number representing the axial flux of swirl momentum divided by axial flux of axial momentum times equivalent nozzle radius *[11]*. The swirl number can be approximated in geometrical terms by Equation 1 *[11, 12]*.

$$SN = \frac{2}{3}\left[\frac{1-\left(\frac{d_h}{d_t}\right)^3}{1-\left(\frac{d_h}{d_t}\right)^2}\right]\tan(\alpha) \quad (1)$$

where, d_h is the hub diameter, d_t is the tip diameter of the swirl and α is the vane angle of swirl.

Experimental Setup of Combustion Performance of the SB Injector

Combustion of Vegetable Oil (VO) using the SB injector

The present study compares the combustion performance of the newly designed SB injector with that of the FB injector using viscous VO as the test fuel. The fuel properties are shown in Table 1 by comparing with diesel and biodiesel, and algae oil *[13]*. The effect of atomizing air to liquid (ALR) ratio across the injector is also investigated to explore the working flow range for the SB injector.

Table 1
Physical and chemical properties of different liquid fuels

Property	Diesel	Biodiesel	Vegetable oil	Algae oil
Chemical formula	$C_{11.125}H_{19.992}$ *[14]*	$C_{18.71}H_{34.71}O_2$ *[15]*	$C_{17.78}H_{32.51}O_2$ *[16]*	-
Density (kg/m^3), 25ºC	834.0 ± 9.2	888.0 ± 8.3	925.0 ± 8.6	938.0
Heating value (MJ/kg)	44.6	37.66	37	37.6
Kinematic viscosity (mm^2/s), 25ºC	3.88 ± 0.02	5.61 ± 0.02	53.74 ± 0.22	TBD
Surface tension, 25 ºC (mN/m)	28.2 ± 0.6	31.1 ± 0.6	30.1 ± 0.6	TBD
Auto-ignition temperature (ºC)	260	177	406	TBD

The novel SB fuel injector consists of a central liquid fuel port and atomizing air is supplied through slots on the circumference of the concentric liquid port. Liquid fuel enters the

injector through a sidewise inlet channel on the injector holder, with the atomizing air supplied through the bottom of the holder. The flow blurring concept is ensured by having a gap of H = 0.25D between the liquid fuel tube tip and the injector orifice with D being 0.06 in. (1.5 mm). The atomizing air leaves the injector exit orifice with a swirling flow through a swirl path generated with an axial curved vane at 70-degree angle with respect to the axial plane giving a swirl number of approximately 2.4.

Figure 3 illustrates the schematics of the experimental setup of the 7-kW lab-scale gas turbine burner with flow lines. The compressed air is split into primary air and atomizing air.

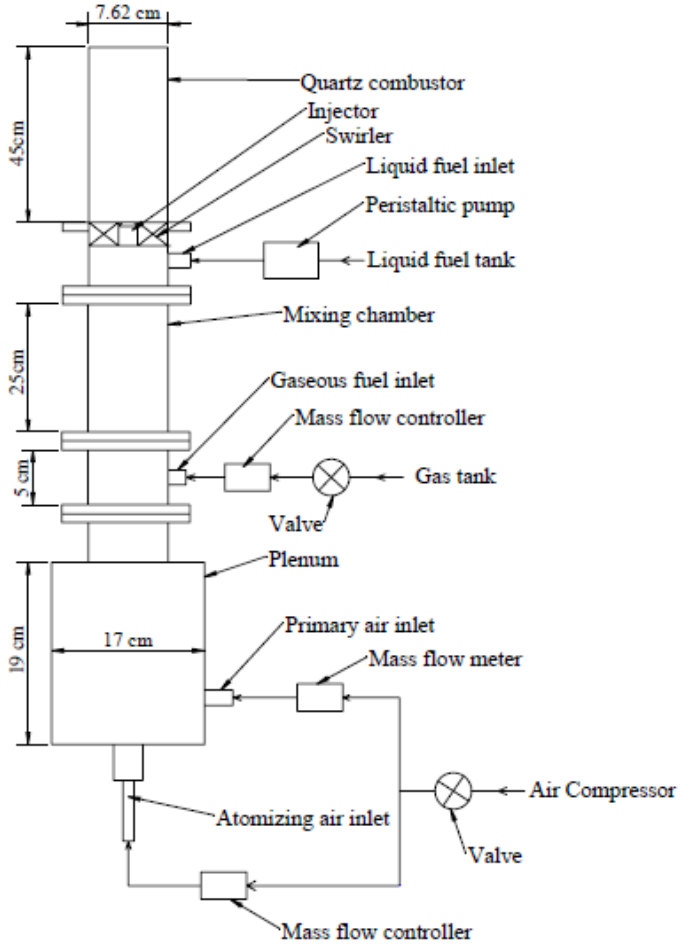

Figure 3

Schematics of Experiment Setup of the Combustion System using the SB or FB injector

The primary air travels through the plenum partially filled with marbles to breakdown the vortical structure and ensure laminar flow into the mixing chamber. Natural gas (NG) is also introduced into the mixing chamber to mix with primary air. Premixed NG and air enters the quartz combustor through a swirler with axial curved vanes at 60-degree angle with respect to the axial plane ensuring a swirl number of approximately 1.5. Combustion of NG was used

to preheat the combustor before completely switching to liquid fuel. The quartz combustor is 3 in. (7.62 cm) in diameter and about 18 in. (45 cm) long. The liquid fuel is delivered by a peristaltic metering pump (Model 75211-70) with an accuracy of ± 0.25 percent of the reading. The primary air flow rate was controlled by a needle valve and measured using a 0-500 liters per minute (lpm) mass flow meter (Omega Model No.: FMA5542A) with an accuracy of ± 1 percent of full scale. The atomizing air flow and NG flow rates were controlled and measured using a 0-50 lpm mass flow controller (Omega Model No: FMA 2609A) with an accuracy of ± 0.3 percent of the reading. Compared to a FB injector, combustion performance including flame images, emissions, gas product temperatures and combustor outside wall surface temperatures were characterized for vegetable oil (soybean oil, about 15 times more viscous than diesel) to investigate the efficacy of the new design. Product gas including carbon dioxide (CO_2), oxygen (O_2), carbon monoxide (CO) and nitrogen oxides (NOx) are sampled continuously at 1 inch upstream of the combustor exit and at 15 radial locations using ENERACTM M500 emission analyzer with an accuracy of ± 2 percent of reading. The temperatures of the product gas at 1 inch upstream of the combustor exit are also measured using this analyzer with an accuracy of ± 2 ^{o}F of reading. The surface temperature of the combustor outside wall were acquired using a high temperature surface thermocouple probe (HPS-HT-K-12-SMP-M) with an accuracy of ± 4 ^{o}F of reading. Experiments were conducted for total air flow rate (combustion air plus atomizing air) of 152 lpm. For a constant Heat release rate (HRR) of 6.7 kW, liquid fuel flow rate of 11.8 mlpm was used for VO. Experiments were conducted for air to liquid mass ratio (ALR) of 3.5 obtained by using the atomizing air flow rate of 32.4 lpm for the injector with and without swirl respectively. Investigation into the effect of ALR on the combustion performance of the SB injector was also carried out using ALRs of 3.0, 3.5 and 4.0.

Effect of SB Injector Geometry on Combustion of Algae Oil (AO)

The present study also characterizes the combustion performance of AO, the third generation of biodiesel source oil, to explore the feasibility of clean direct combustion of AO, saving the converting cost and energy. This work investigates the effect of the SB injector geometry in terms of varying swirl numbers, i.e., different swirl vane angles. The SB injector integrates the FB concept with D of 0.06 in. (1.5 mm) and a gap of H = 0.25D between the liquid fuel tube tip and the injector orifice. The atomizing air leaves the injector exit orifice with a swirling flow through a swirl path generated with an axial curved vane at 60, 65 and 70-degree angle with respect to the axial plane giving swirl numbers of approximately 1.5, 2.0 and 2.4 respectively. The same combustion system shown in Figure 3 is used for the investigation.

Combustion performance including flame images, emissions, gas product temperatures and

combustor outside wall surface temperatures were characterized for algae oil flame to investigate the efficacy of the new design and effect of vane angles. Product gas including carbon dioxide (CO_2), oxygen (O_2), carbon monoxide (CO) and nitrogen oxides (NOx) are sampled continuously at 1 inch upstream of the combustor exit and at 15 radial locations using ENERAC^{TM} M500 emission analyzer with an accuracy of ± 2 percent of reading. The temperatures of the product gas at 1 inch upstream of the combustor exit are also measured using this analyzer with an accuracy of ± 2 ^{o}F of reading. The surface temperature of the combustor outside wall were acquired using a high temperature surface thermocouple probe (HPS-HT-K-12-SMP-M) with an accuracy of ± 4 ^{o}F of reading. Experiments were conducted for total air flow rate (combustion air plus atomizing air) of 150 lpm. For a constant Heat release rate (HRR) of 6.6 kW, liquid fuel flow rate of 11.3 mlpm was used for AO. Experiments were conducted for air to liquid mass ratio (ALR) of 4.0 obtained by using the atomizing air flow rate of 37.8 lpm for the SB injectors with different swirl numbers.

Spray Characterization using Particle Image Velocimetry (PIV)

Experimental Setup of the Spray Injection System

In this study, a new internally-mixing twin-fluid SB injector and a FB injector are utilized. A FB injector with diameter of liquid tube and exit orifice of 0.06 in (1.5 mm) is employed. The FB injector has the gap between the tip of liquid tube and the exit orifice of 0.015 in (0.375 mm). The SB injector has the same dimensions with FB injector with a swirl number of approximately 2.4. Figure 4 depicts the schematic of the injection system used in this study. In this experiment, water and air are used as the working fluids. A Cole Parmer pump (Model 75211-70) with accuracy of ± 0.25% of reading is used to supply the liquid and adjust the flow rate to the FB and SB injectors. AA flow rate is controlled by an Omega mass flow controller (Model FMA – 2600A) with an accuracy of ± 0.3% of reading. Water enters the injectors with flow rate of 12 ml/min. AA is supplied to the system at 15 standard liters per minute to obtain an air to liquid mass ratio (ALR) of 1.5.

The project examines the pressure drop in AA and liquid lines across injectors to compare energy input needed for AB, FB, and SB injectors. Two pressure transducers (Model PX309) with 0.25% static accuracy are installed upstream of the injectors in AA and liquid lines. Mass flow rate of water is kept constant at 12 ml/min. AA varies from 1 to 2.5 slpm, yielding ALR of 1 to 2.5.

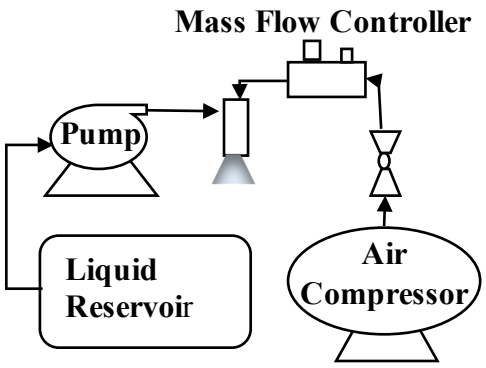

Figure 4
Injection system

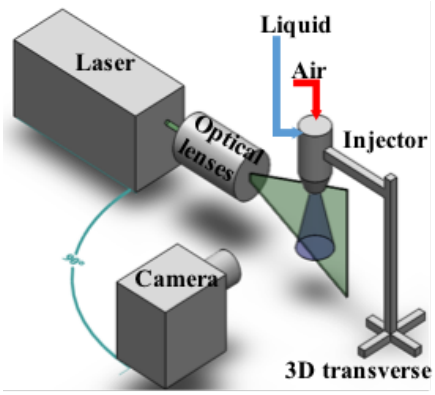

Figure 5
PIV experimental setup

Particle image velocimetry (PIV) Setup and Data Processing

A PIV system as shown in Figure 5 is utilized to measure droplet velocity field of FB and SB sprays. A dual head Nd: YAG laser operating at 532nm wavelength is used to generate two laser pulses with pulse separation of 0.5 µs at 15 Hz pulse repetition rate. The ultra-short laser pulse duration of 4 ns freezes fast-moving droplets of sprays and thus resolves the spray dynamics. A divergent laser sheet optics consisted of a – 0.59 in (15 mm) focal-length cylindrical lens and a 39.37 in (1000 mm) spherical lens formed a 0.04 in thick laser sheet to illuminate the field of view (FOV). A Tokina lens (Model Macro D) with 3.94 in (100 mm) focal length and f-number of 2.8 is mounted on a 4MP-LS camera (Model 630090) which perpendicularly focused on the laser sheet with spatial resolution of 7.14 µm per pixel. The camera synchronized with the dual head laser head captured two consecutive single-exposure images to acquire frame-straddle image pair with the time interval of 0.5 µs at 15 Hz, i.e 30 frames per second (fps).

Insight 4G software is employed to acquire two consecutive single exposure images in frame-straddle mode with the cross-correlated sub-region of image pairs to generate the velocity vectors of the near-field FB and SB sprays. To obtain nearly 100% valid velocity measurements, initial interrogation window size of 64 pixels by 64 pixels with 50% overlap spacing are selected in Insight 4G to minimize the particle-correlation noise and ensure more than ten effective particle pairs in each interrogation window *[17]*. The effects of out-of-plane motion on the accuracy of the velocity measurements are neglected due to the ratio of out-of-plane displacement to the light sheet thickness is about 0.005 which is much less than the maximum acceptable level of 0.25 *[17]*. Signal to noise ratio is set to be greater than 1.4

to eliminate inauthentic vectors. Signal to noise ratio is the ratio of the displacement peak, which is the highest peak, to the noise peak, i.e., the second highest peak. After signal to noise ratio test, median test is applied to eliminate more inauthentic vectors. An error velocity vector is replaced by a valid secondary peak at the same spot when the difference between the velocity vector and the local median vector exceeds the tolerance of 2 pixels.

DISCUSSION OF RESULTS

Combustion Performance of the SB injector on Vegetable Oil (VO)

Effect of Swirling Atomizing Air

Figures 6(a) and (b) show the visual flame images of straight vegetable oil (VO) using flow blurring (FB) and swirl burst (SB) injectors respectively at the same fuel flow and air flow rates. The dominant blue color of the flames indicates that clean and complete combustion of the hydrocarbons (CH-chemiluminescence) has been achieved for viscous VO for both injectors. The dark regions upstream of the FB and SB flames indicate fuel pre-vaporization and fuel-air mixing zone, signifying clean mainly lean-premixed (LPM) combustion is acquired for both injectors because of the fine atomization of the two novel injectors. The dark zone of FB spray combustion is about 2.55 in. (7 cm) long starting from the injector exit, shown in Figure 6(a). Interestingly, the fuel pre-vaporization zone in the SB injector is around 1.18 in. (3 cm), almost one-third of that in the FB injector. Three possible reasons can explain the shorter SB fuel pre-vaporization zone. First, the swirling atomizing air (SAA) likely enhances secondary breakup to produce finer droplets, which evaporate faster. Second, improved fuel-air mixing by SAA and thus more heat transfer occurs between fuel droplets and the thermal feedback from the reaction zone to speed up fuel evaporation. Third, decreased axial velocity of SB fuel droplets because of the imposed radial velocity by the SAA in SB injection results in shorter residence distance for the droplet lifetime. Too-lifted flames suffer the possibility of blow-off, especially for long operation period in real applications, resulting in flame instabilities. Less lifted SB flame could better sustain the flames with sufficient thermal feedback to rapidly vaporize incoming droplets and thus achieve clean LPM combustion. Also, Figure 6(b) shows that SB injection results in a slightly more compact flame with length of about 9.05 in. (23 cm) compared to 9.84 in. (25 cm) of the FB spray flame. This can be conformably attributed to quicker fuel evaporation, more thorough fuel-air mixing, and hence, faster fuel oxidation indicative of a shorter reaction zone compared to that of the FB injector. Figure 7 depicts the surface temperature profile of the quartz combustor outside wall for both injectors. Surface temperature increases closer to the injector side indicating the fuel oxidation process along the axial location of the combustor. The combustor wall temperature peaks at approximately 7.87 in. (20 cm) downstream of the injector exit and at around 5.91 in. (15 cm) respectively for the FB and SB flames, substantiating the high-temperature reaction zone at the mid of the flame length as shown in the visual flame images, where the bulk chemical energy is released. The surface temperature at the fuel evaporation zone and reaction zone (0- 21 cm) is higher for the SB injector compared to the FB injector. This can again be attributed to the faster and shorter

fuel evaporation zone with higher thermal feedback for the SB injector, and thus, quicker fuel oxidation and shorter flame length, resulting in higher local temperature in the SB reaction zone at the same heat release rate (HRR) for both test cases. Downstream of the reaction zone, the surface temperature decreases gradually signifying heat loss rate to the surrounding exceeding heat released due to the gradual completion of fuel oxidation and the homogenous thermal mixing of combustion products. The overlapped temperature profiles at downstream of the flames signify that complete combustion has been achieved for both novel injectors at the constant input HRR for the viscous VO.

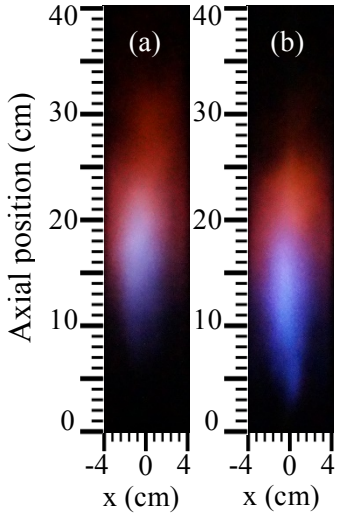

Figure 6
Flame images of the combustion of VO at ALR = 3.5 for (a) FB (b) SB injector

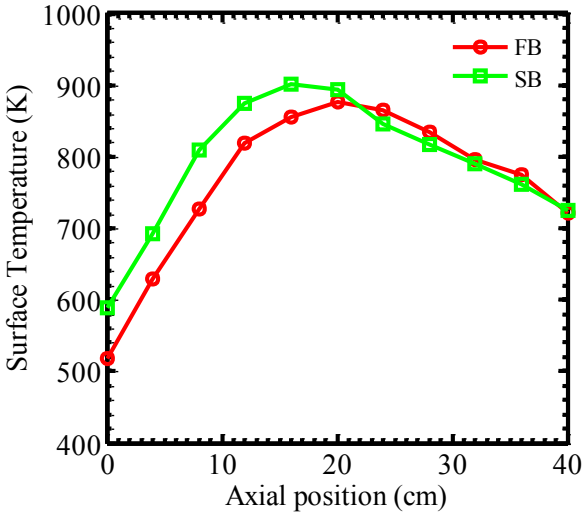

Figure 7
Temperature distribution of combustor outside wall

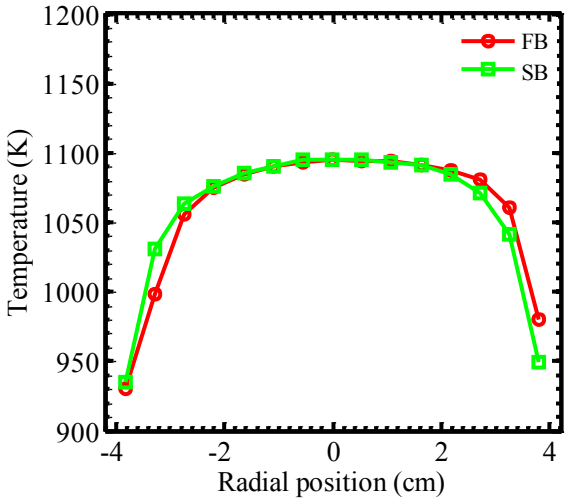

Figure 8
Radial profile of product gas temperature at the combustor exit

Figure 8 outlines the radial profile of the product gas temperature (uncorrected) at the combustor exit plane for FB and SB injectors. The overlapping profile of the product gas temperature obtained from both injectors is testament of the same HRR used in both cases. This coherently signifies the complete combustion of the straight VO using both injectors. The symmetric profile obtained with the SB injector can be attributed to better uniform fuel-air mixture and possibly even droplet size distribution by the SAA on secondary atomization. The low temperature obtained at the walls of the combustor can be explained by the heat loss through the quartz combustor to the ambient via convective and radiative heat transfer.

Figure 9 illustrates the radial profile of CO emissions at the combustor exit for FB and SB injector at the same ALR and HRR. Both injectors produced low emissions of CO from combustion of highly viscous fluid such as VO, indicating the supreme atomization capability and thus, clean combustion of viscous fuels. The CO emissions (11-16 ppm) from the SB injector are slightly higher than those from FB injector (10 ppm). The slight increase can be likely attributed to the higher local temperature in the SB reaction zone yielding mildly higher CO concentration, in consistent with the flame images and surface temperature profiles.

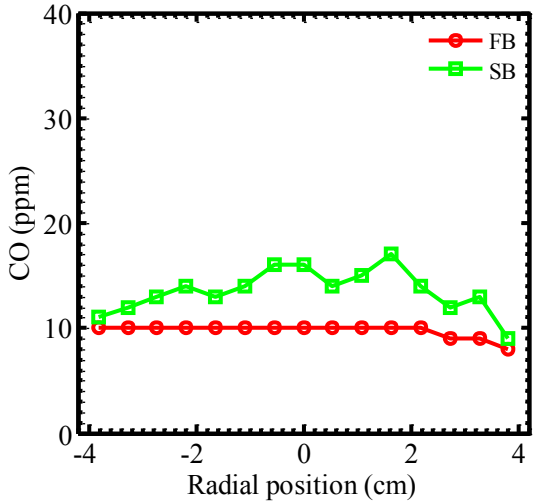

Figure 9
Radial profile of CO emissions

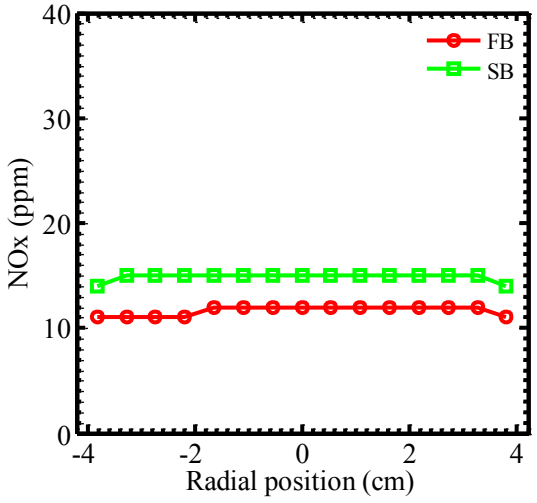

Figure 10
Radial profile of NOx emissions

Figure 10 shows the radial profile of NOx emissions, at the combustor exit, of straight VO using FB and SB injectors. Both injection methods generated low NOx emissions (< 15 ppm) especially considering the high viscosity of straight VO (about 15 times more viscous than diesel), signifying the excellent performance of the injectors in the clean lean premixed combustion of straight VO. Without the fuel nitrogen, NOx is mainly generated by the thermal NOx mechanism which effects at temperatures above 1800 K. Future test could

further lower the NOx emissions by using lower equivalence ratio, i.e. fuel leaner combustion. The NOx emissions obtained from the SB injector is about 4 ppm higher than those from the FB injector. This can be consistently attributed to the locally higher temperature within the reaction zone to give slightly higher thermal NOx. Overall, both injectors resulted in relatively low NOx emissions for viscous VO, about 0-15 ppm, despite the slight difference.

Effect of atomizing air to liquid mass ratio (ALR) of the SB Injector

The present study also investigates the effect of ALR to explore the optimum flow range for the SB injector with swirl number (SN) of 2.4 at the constant HRR of 6.8 kW for straight VO, yielding the fuel flow rate of 11.8 milliliters per minute (mlpm). The investigation includes ALRs of 3.0, 3.5 and 4.0 by varying the flow rate of the atomizing air (AA).

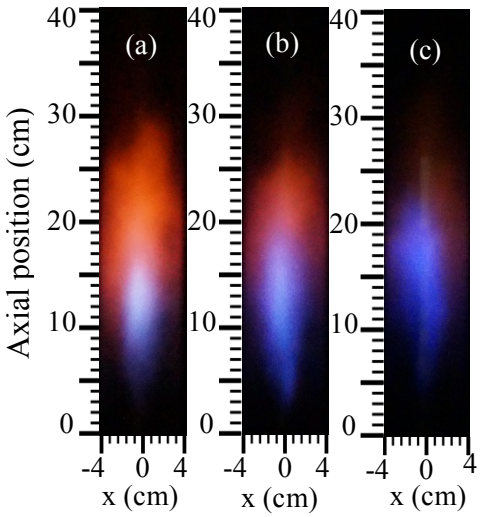

Figure 11
Flame images of the combustion of VO using SB injector at ALRs of (a) 3.0 (b) 3.5 (c) 4.0

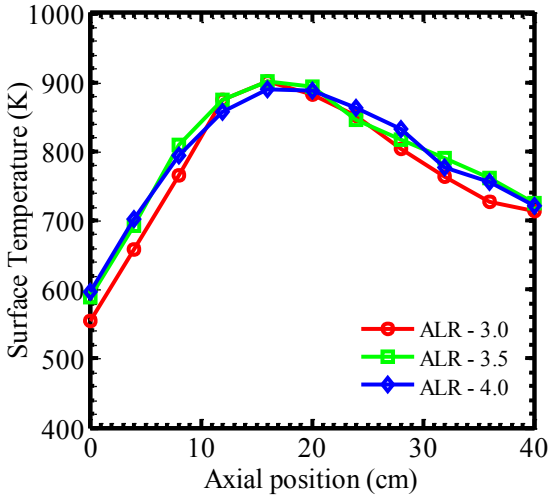

Figure 12
Temperature distribution of combustor outside wall at various ALRs

Figure 11 shows the visual flame images from the combustion of straight VO using the SB injector at varying ALRs. The flame images are similar qualitatively with minor visual differences. The flame color becomes dominantly blue with increase in ALR which can be ascribed to finer droplets evolution at higher ALR aiding fast and complete pre-vaporization and fuel air mixing, hence cleaner combustion. Figure 11(a) is the flame image for ALR of 3.0 having an upstream dark zone, i.e. fuel pre-vaporization and fuel-air mixing zone, with length of about 2.36 in. (6 cm) downstream of the injector exit plane. ALR of 3.5 in Figure

11(b) has a shorter dark region upstream of the flame with length of about 1.18 in. (3 cm) from the injector exit plane. This difference can be attributed to faster evaporation of finer droplets at higher ALR of 3.5 yielding a less lifted flame to that in Figure 11(a). Interestingly, in Figure 11(c), the adverse tendency of flame lifting length occurs with the further increase in ALR to 4.0 which has a more lifted blue flame with fuel-prevaporization zone about 2.36 in. (6 cm) long. This result can be attributed to the faster-moving finer droplets carried by the increased AA velocity. Consistently, the shorter flame length at ALR of 4.0 is due to the finer droplets obtained at higher ALR, coupled with enhanced secondary atomization provided by the SB effect, hence quickly evaporating and mixing well with air, yielding fast fuel oxidation.

Figure 12 depicts the surface temperature distribution of the combustor outside walls at the investigated ALRs. The surface temperature typically increases along the flow (axial) direction to a peak and gradually reduces further downstream. The slightly lower surface temperature near the dump plane at ALR of 3.0 corroborates the lifted flame obtained at this ALR. Interestingly, the peak of the surface temperature profile coincides for all the ALRs at about 5.91 in. (15 cm) downstream of the injector exit plane. This signifies relatively close reaction zone obtained with the SB injector at different ALRs.

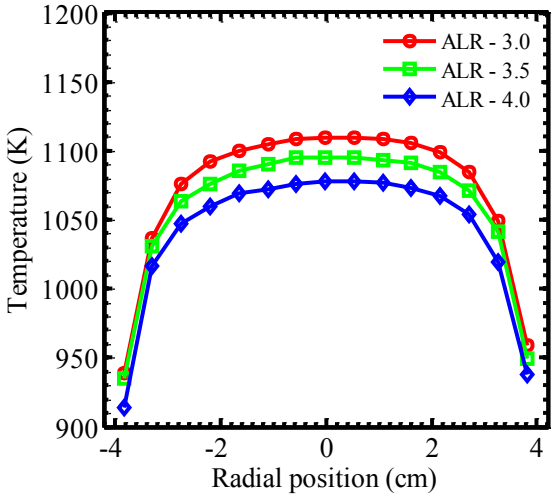

Figure 13

Radial profile of product gas temperature of SB injector at different ALRs

Figure 13 shows the radial profile of the product gas temperature (uncorrected) at the combustor exit plane from the combustion of VO using SB injector at different ALRs. The symmetric profile of the product gas temperature is apparent across all ALRs validating the ability of the SB injector in achieving better uniform fuel-air mixture and even droplet size distribution as discussed above. The product gas temperature at the combustor exit plane

decreases as the ALR increases. This may be attributed to the reason that for the same HRR, compact flames at increased ALRs hence shorter reaction zones yield higher local temperature and thus more significant thermal radiation heat loss to the surrounding. This ultimately results in the low product gas temperature measured at the combustor exit plane. The low temperature obtained at the walls of the combustor can be attributed to the heat loss through the quartz combustor to the ambient via convective and radiative heat loss.

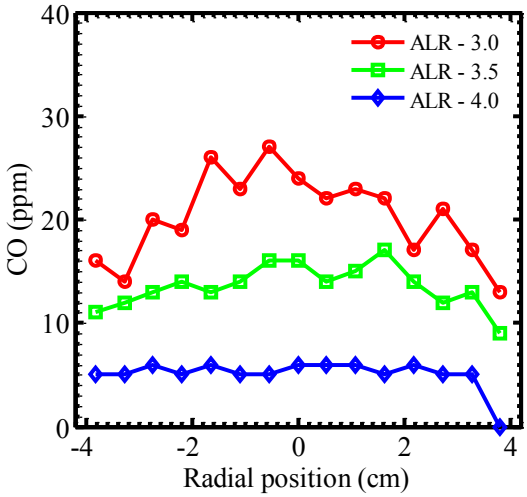

Figure 14
Radial profile of CO emissions of SB injector at different ALRs

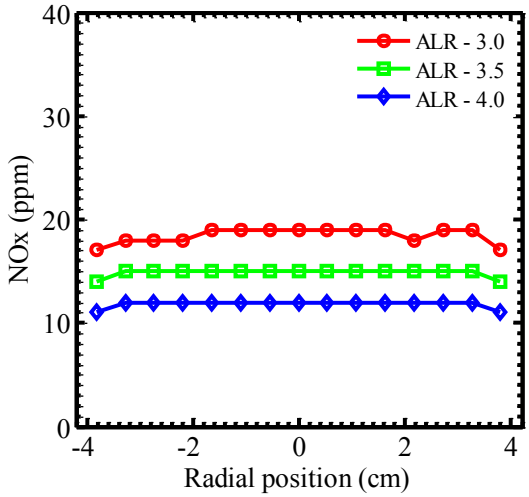

Figure 15
Radial profile of NOx emissions of SB injector at different ALRs

Figure 14 outlines the radial profile of the CO emissions at the combustor exit from combustion of VO using the SB injector at different ALRs. The CO emission obtained at ALR of 3.0 was about 15-26 ppm, 11-16 ppm for ALR of 3.5 and 0-5 ppm for ALR at 4.0. The difference in the CO emissions obtained at different ALRs can be attributed to enhanced fuel atomization by the FB concept within the SB injector at higher AA flow rates with the SB concept enhancing the secondary atomization through shorter pre-vaporization and improved fuel air mixing. Some relatively larger droplets penetrate into the reaction zone without thorough evaporation burning at diffusion mode and thus yielding slightly higher CO concentration. The CO emissions are typically lower at the combustor walls for all the ALRs which is likely because the swirling combustion air further disintegrating the fuel droplets at the periphery of the spray coupled with the thermal feedback from the combusted product for fast fuel vaporization and complete burning at clean lean-premixed mode. Overall, the SB injector achieved clean mainly LPM combustion of viscous VO across all ALRs and ALR of 4.0 gave the cleanest emissions.

Figure 15 illustrates the radial profile of the NOx emissions at the combustor exit from burning straight VO using the SB injector at different ALRs. Ultra-low NOx emissions, within 10-20 ppm, were obtained at all ALRs signifying the excellent ability of the SB injector to achieve clean combustion of viscous VO. Decrease in ALR resulted in higher NOx concentrations, signifying relatively larger droplets at lower ALR burning at diffusion mode with higher local temperature, and thus, higher thermal NOx. ALR of 4.0 also achieved the lowest NOx emissions, about 0-10 ppm, which can be attributed to more efficient atomization at higher ALRs and lower local temperatures of LPM combustion resulting in low thermal NOx formation.

Effect of the SB Injector Geometry on Combustion of Algae Oil

The current work investigates the possibility of direct combustion of algae oil with low emissions using the SB injector. Parametric study of the effect of injector swirl number with varying vane angles has been conducted at the constant flow rates and ALR of 4.0, which has been proved to yield ultra-low emissions as discussed above.

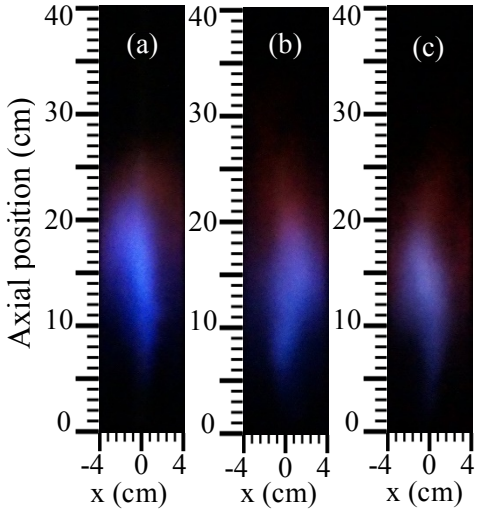

Figure 16
AO Flame images using SB injector at ALR = 4.0 with SN (a) 1.5 (b) 2.0 (c) 2.4

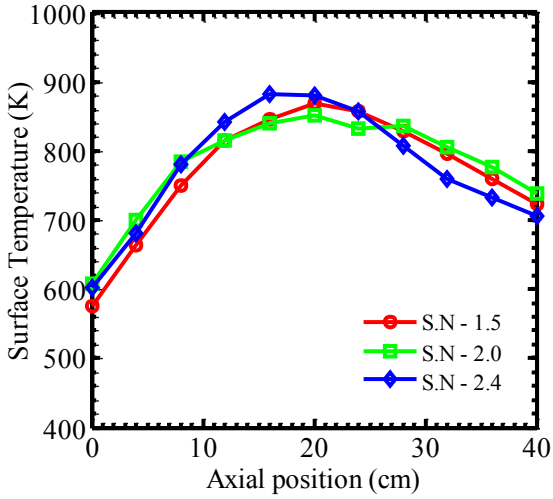

Figure 17
Axial profile of combustor outside wall temperature for SB injector with varying swirl number

Figure 16 depicts the visual flame images of the combustion of algae oil (AO) using the swirl burst injectors with different swirl numbers (SN) at ALR of 4.0 and constant flow rates. The dominant blue color of the flame images signifies clean complete combustion of the hydrocarbons (CH-chemiluminescence). The dark regions upstream of flames for all the three test cases signify fuel pre-vaporization and fuel-air mixing before fuel oxidation, indicating mainly premixed combustion achieved for all SNs because of the superior SB

atomization capability. Figures 16(a-c) show dark zone length of approximately 2.76 in. (7 cm), 2.36 in. (6 cm) and 1.97 in (5 cm) upstream of the flames, respectively for the injector with SN of 1.5, 2.0 and 2.4. The slight decline in the length of fuel pre-vaporization zone with the increasing SN, i.e. bigger injector swirling vane angles, can be likely explained by (a) the finer droplets, and (2) enhanced thermal mixing by the increased radial velocity component of the SAA for higher SN, and (3) reduced droplet axial velocity leading to shorter residence distance for droplet evaporation. The increasing momentum of SAA in the radial direction for higher SN results in more vigorous interaction between the SAA and the relatively larger droplets from primary bubble bursting, hence generating smaller droplets immediately at the injector exit with faster fuel evaporation. The increased radial momentum of SAA also enhances the fuel-air mixing with the thermal feedback from combustion gas products, further quickening the fuel vaporization, followed by faster fuel oxidation [24, 26]. As the result, slightly shorter flame of approximately 6.69 in. (17 cm (5-22 cm)) at the increased SN of 2.4 as shown in Figure 16(c), compared to that of 7.07 in. (18 cm) for SNs of 2.0 and 1.5 with flame located at axial location of 2.76-9.84 in (7-25 cm) and 2.36-9.45 in (6-24 cm) respectively in Figures 16(a-b). The nearly same flame length for SNs of 2.0 and 1.5 is likely the combining effect of smaller droplet size and lower axial velocity at the increased SN of 2.0.

Figure 17 shows the temperature distribution of the combustor outside wall for AO using the SB injector with different injector swirl numbers. The temperature profile increases in the flow direction and reaches a peak before decreasing further downstream, signifying the fuel evaporation, fuel oxidation achieving highest temperature, followed by lower temperatures because of the complete combustion and products mixing. The surface temperatures of SN of 2.4 are slightly higher than those of SN of 1.5 and 2.0 at around axial location of 3.94-9.06 in (10 – 23 cm), where the center reaction zone releases bulk chemical energy. The discrepancy can be ascribed to the shorter flame leading to higher reaction zone temperatures at the same HRR for the increased SN. In regardless of the slight variation in reaction zone, the nearly overlapped temperature profiles of all three SNs indicate that complete combustion of straight AO irrespective of swirl number using the SB injection without fuel preheating.

Figure 18 illustrates the radial profile of CO emissions at the combustor exit from the combustion of AO using the SB injector with different SNs. Amazingly, nearly none CO emissions of straight AO without fuel preheating are detected at the combustor exit for all the investigated SNs. This result consistently indicates that the complete and clean combustion of straight AO has been achieved owing to the further enhanced atomization capability of the SB injector and thus improved fast vaporization, better fuel-air mixing, hence the clean premixed flames. Figure 19 depicts the radial profile of NOx emissions at the combustor exit from the combustion of pure algae oil using the SB injector with different SNs. The SB

injectors produced ultra-low NOx emission in the range of 5-10 ppm further validating the ability of the SB injector to achieve clean combustion of heavy and viscous AO. The SB injector with SN of 2.4 interestingly produced higher NOx emission of about 10 ppm compared to the injector with SN of 2.0 that had about 5 ppm. This can be attributed to locally higher reaction zone temperature as discussed above, thereby producing higher local thermal NOx formation. At the low SN of 1.5, i.e. less SAA effect, some relatively larger droplets might penetrate into reaction zone with the higher axial velocity and burn at diffusion mode yielding slightly higher local temperature, as shown in Figure 17, and thus higher thermal NOx. Despite this, the SB injectors produce low NOx emissions less than 10 ppm thus clean and complete combustion of AO. In summary, SN of 2.0 yields the lowest NOx emissions by the combined benefit of enhanced atomization and appropriate axial velocity to achieve less lifted flame with lower local reaction temperature and thus minimize thermal NOx.

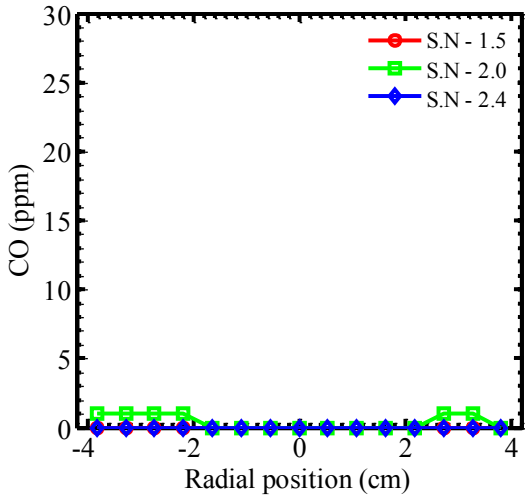

Figure 18
Radial profile of CO emissions for SB injector with varying swirl number

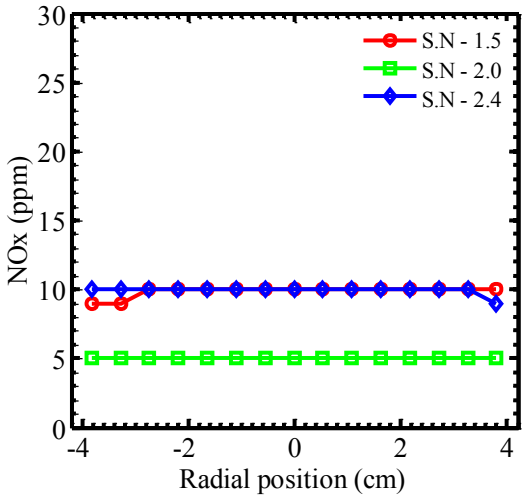

Figure 19
Radial profile of NOx emissions for SB injector with varying swirl number

Figure 20 illustrates the radial profile of the product gas temperature at the combustor exit from the burning of AO using the SB injectors with different SNs. The nearly overlapping product gas temperature profile can be explained by the same HRR used for the three test cases, consistently substantiating the clean and complete combustion of pure AO within the combustor. The symmetric profile of the product gas temperature consistently signifies the uniformity of the fuel air mixture and even droplet size distribution achieved by the swirling secondary atomizing air of the SB injector. The lower temperatures obtained at the combustor walls consistently validates the heat loss to the surrounding through the combustor

wall from convective and radiative heat loss. Overall, clean premixed combustion of straight AO has been achieved using the novel SB injector.

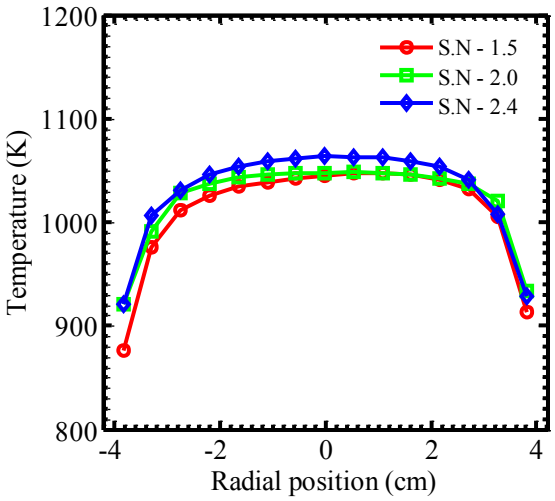

Figure 20
Radial profile of product gas temperature for SB injector with varying swirl number

Comparison of Spray Characteristics of SB and FB injectors

The present study gains insight into the spray features in the near field of the SB injector as compared to those of the FB injection using the high spatial resolution PIV system. Figures 21(a) and 21(b) show the PIV spray images in the injector near field with FOV of 0.39 in (10 mm) by 0.39 in (10 mm) at spatial resolution of 7.14 μm per pixel for FB and SB injectors, respectively. White dots in the images represent atomized water droplets, surfaces of which scatter the incoming laser light into the camera sensor to form the spray images. The PIV laser with short pulse duration of 4 ns, i.e. the image exposure time, freezes the fast-moving droplets. Majority of droplets near the exit orifice plane in both images are fine droplets ranging from around 28 μm in diameter with the maximum of about 107 μm, revealing the effective primary atomization by bubble bursting occurred slightly upstream of FB and SB injector exits (y = 0 in). Compared to the FB spray at the injector near field (within 1 in downstream of the injector exit), less bright spots in Figure 21(b) signify that finer droplets with less reflected light are formed by the SB injector. This can be attributed to the enhanced secondary atomization by the swirling atomizing air, which rapidly disintegrates the relatively larger droplets into fine ones in SB atomization. At further downstream, the SB spray contains only fine droplets while few larger droplets are observed at periphery of FB sprays. This comparison indicates that atomization is almost completed at the axial location of 0.08 in (2 mm) downstream of the SB injector orifice, indicating the further improved

atomization capability and thus resulting in fast fuel evaporation and fuel-air mixing for efficient and clean combustion in real applications.

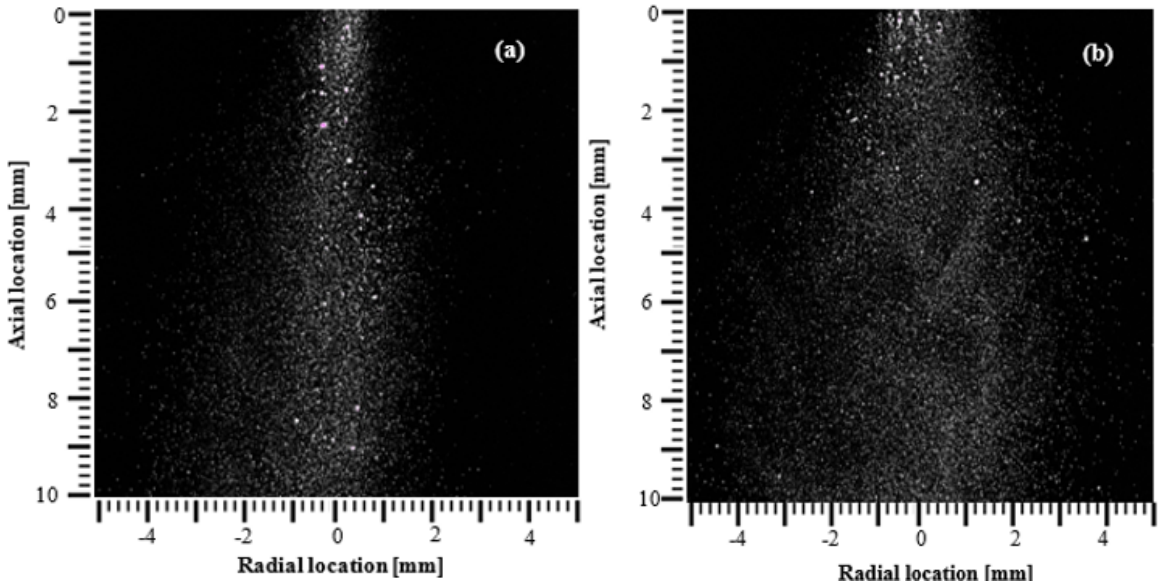

Figure 21

Water spray image of (a) FB injector, (b) SB injector at the injector near field with the FOV of 10mm by 10mm

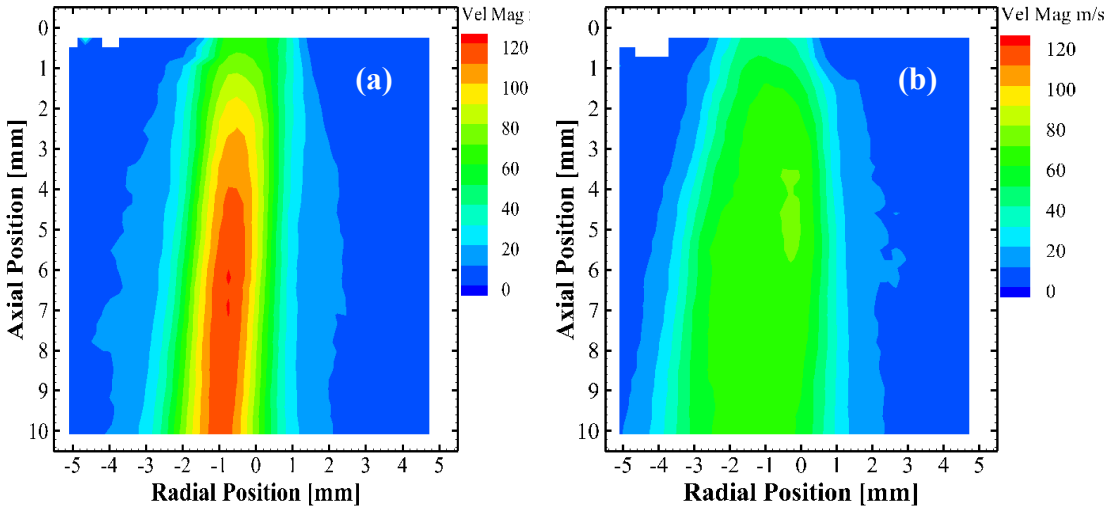

Figure 22

Time-averaged field of droplet velocity magnitude contours for (a) FB injector, (b) SB injector

Figure 22 shows the ensemble average field of droplet velocity magnitude for FB and SB sprays at the same flow conditions computed from 500 instantaneous velocity vector fields

using Insight 4G and Tecplot Focus PIV. Previous FB spray characterization using PIV by Jiang and Agrawal (2014 & 2015) *[7, 8]* revealed the inverse relationship between droplet size and velocity. At the same flow conditions and injector geometry, finer droplets tend to streamline with the high-velocity atomizing air and move at a faster speed. Jiang and Agrawal (2014 & 2015) *[7, 8]* also found that the velocity variation reflected the size change in droplets, signifying the ongoing atomization process. Figure 22 shows that droplets from both FB and SB sprays accelerated with flow direction indicating further breakup of relatively larger droplets from the primary atomization. Interestingly, droplets velocity from SB sprays in Figure 22(b) remained constant after 0.06 in (1.5 mm) downstream from the exit orifice plane, while this phenomenon occurred at about 0.16 in (4 mm) downstream for the FB injector. This signified the improved secondary atomization of SB injector, which is consistent with the visual spray images in Figure 21.

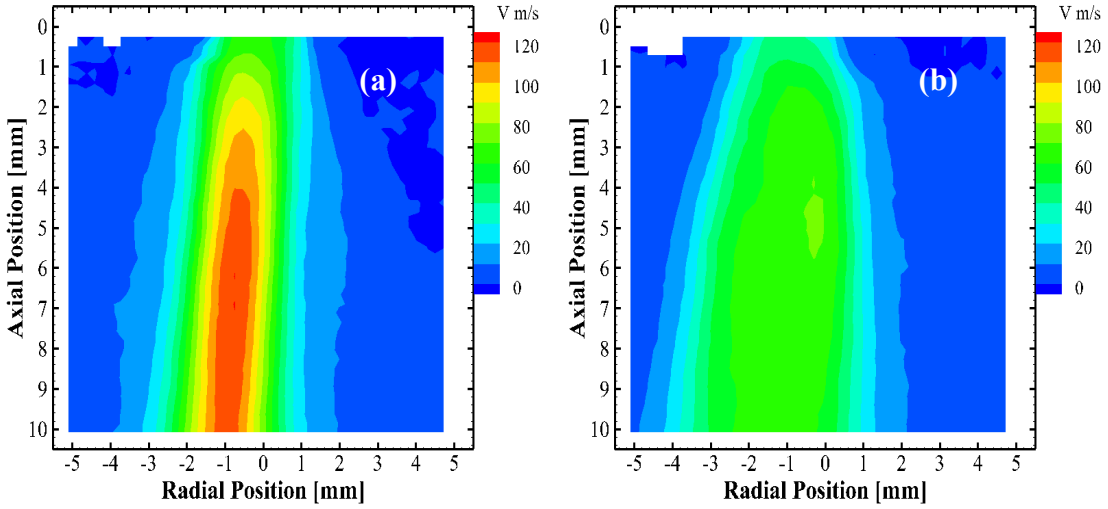

Figure 23
Time-average field of droplet axial velocity for (a) FB injector, (b) SB injector

Figure 23 shows the average droplet axial velocity for the tested injectors. The highest velocity of droplets generated from the SB injector is about 262 ft/s (80 m/s) while the peak droplet velocity of FB spray is about 394 ft/s (120 m/s). This can be attributed to the swirling path on the injector head as shown in Figure 2, which introduced the AA leaving the injector exit with higher radial velocity component and thus improved the interaction between the escaping air and larger droplets mainly at the spray periphery. The enhanced interaction harnessed more kinetic energy of the high-velocity air to overcome the surface tension of the droplets and disintegrate them into smaller ones, effectively facilitating the secondary atomization of SB injection. Compared to FB injection, fine spray with lower droplet velocity of SB injection ensures long-enough residence time for fuel pre-evaporation, fuel-air

mixing, fuel oxidation and thus clean and efficient combustion. The similarity of the axial velocity profile in Figure 23 and the spray velocity magnitude in Figure 22 indicates that the axial velocity dominates the spray flow field for both injectors, though radial velocity component is more effective in the SB injector to enhance the secondary droplet disintegration, as shown in Figure 24. Droplets generated from FB injectors and SB injectors have high axial velocity at the center and decrease in radial direction shown in Figures 23(a) and 7(b), respectively, showing the typical radial expansion of fuel sprays. The wider SB spray in Figure 23(b) again indicated the higher radial velocity because of the swirling atomizing air. Figure 24 quantitatively revealed the higher velocity component of the SB spray in the radial direction than that of the FB spray.

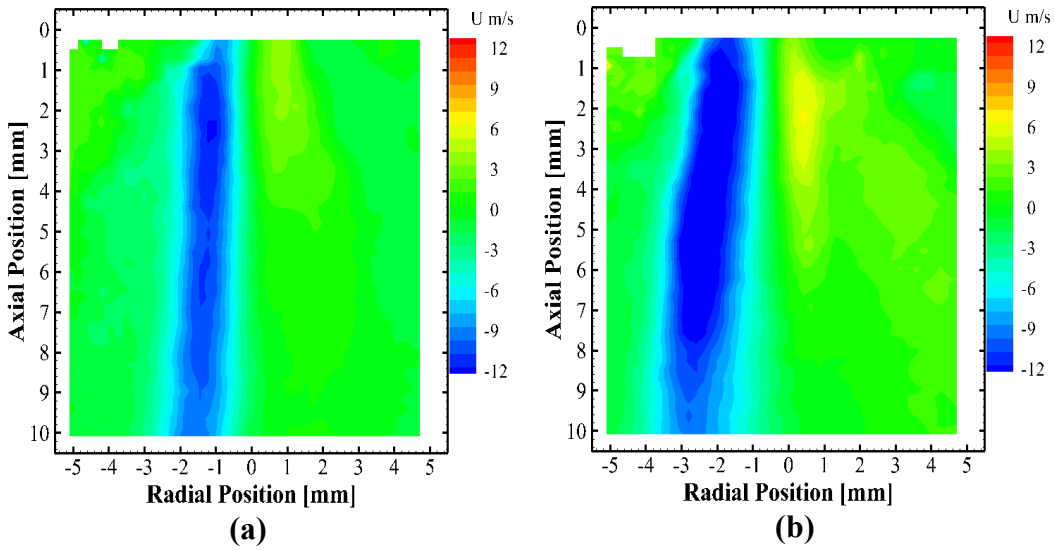

Figure 24
Time-average field of droplet radial velocity for (a) FB injector, (b) SB injector

Figures 25 and 26 show the radial profile of the droplet axial velocity and radial velocity, respectively, at various axial locations downstream of the injector exit (y = 0 in). The figures quantitatively illustrate the dynamic evolution of the FB and SB sprays along flow direction. The peak axial velocity of droplets gradually increased with the axial locations from 0.02 in (0.5 mm) to 0.24 in (6 mm) for the FB spray shown in Figure 25(a). At the axial location of 0.02 in (0.5 mm), the highest droplets velocity from FB sprays is around 197 ft/s (60 m/s).

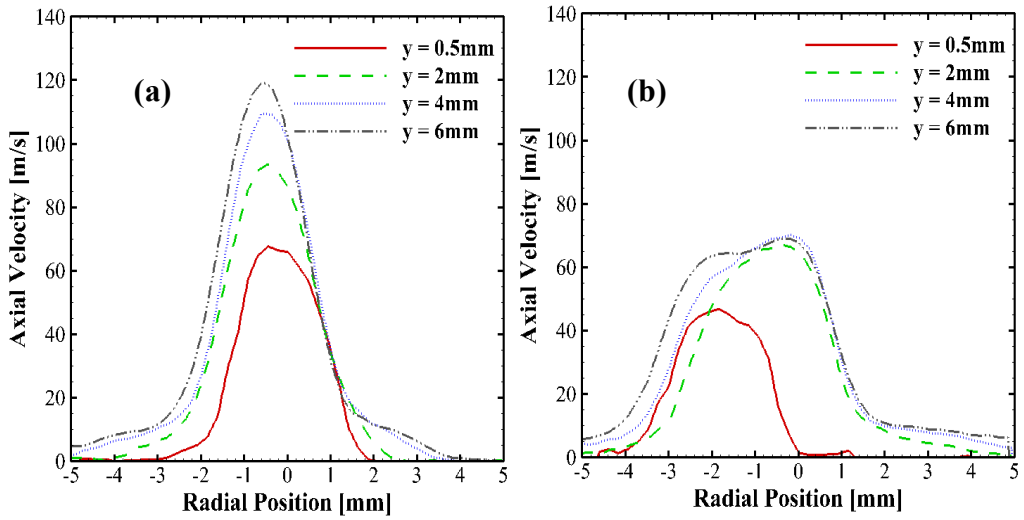

Figure 25

Droplet axial velocity profile of time-average for (a) FB injector, (b) SB injector

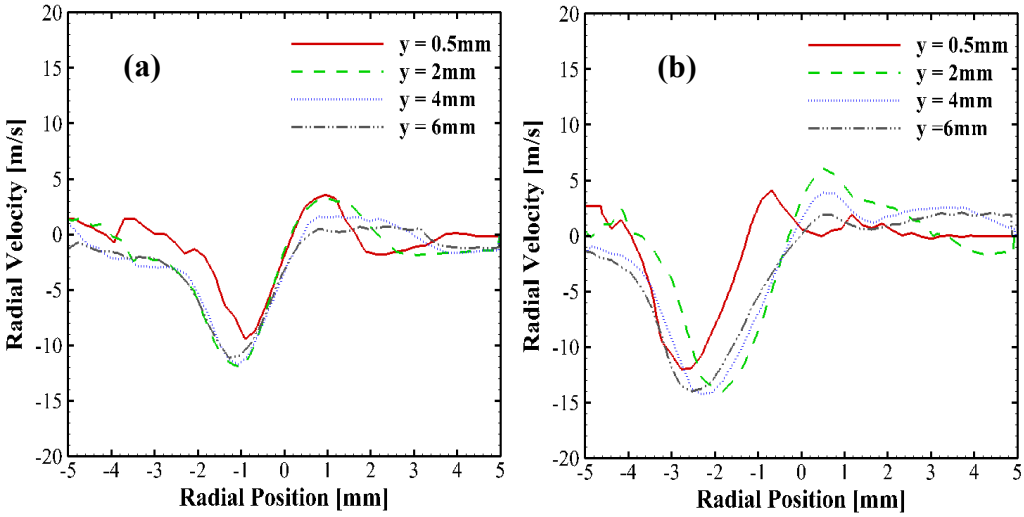

Figure 26

Droplet radial velocity profile of time-average for (a) FB injector, (b) SB injector

The peak velocity of the droplets increased to about 295 ft/s (90 m/s), 361 ft/s (110 m/s), and 394 ft/s (120 m/s) at the axial locations of y = 0.08 in (2 mm), 0.16 in (4 mm), and 0.24 in (6 mm), respectively, indicating the ongoing secondary droplet breakup. However, the axial velocity profiles of the SB spray, shown in Figure 25(b), were almost overlapped on one another at the axial location of 0.08 in, 0.16 in, and 0.24 in. This consistently indicated the complete SB atomization at around 0.08 in (2 mm) downstream the injector orifice due to the enhanced secondary droplet breakup. The axial velocity profiles of FB sprays in Figure 25(a) evince that droplets of higher velocity are concentrated around the center (x = 0 in) of spray

from x = – 0.02 in (- 0.5 mm) to 0.02 in. In contrast, in Figure 25(b), the higher-velocity droplets spread out from x = -0.08 in (- 2 mm) to 0.02 in (0.5 mm) in SB spray, consistently showing majority of larger droplets at periphery region from primary bubble bursting have been disintegrated into finer drops with faster speed at downstream of 0.08 in (2 mm) by the improved secondary atomization. The radial velocity profiles at different axial locations are shown in Figure 26. The maximum radial velocity of FB spray is around 33 ft/s (10 m/s) as shown in Figure 26(a) while SB droplet radial velocity peaked at around 49 ft/s (15 m/s) as shown in Figure 26(b), resulting in the more vigorous secondary breakup by increased shear layer instabilities in the radial direction between the swirling air and larger droplets.

Figure 27 shows temporal profile of axial droplet velocity at the spray center at different axial locations for FB and SB injectors for the 500 consecutive velocity fields measured at 15 Hz. The FB injector generated droplets velocity at least 66 ft/s (20 m/s) higher than droplets velocity generated by the SB injector because of the higher radial droplet velocity by the swirling effect as aforementioned. For the FB injection in Figures 27(a-d), at all the tested axial positions, the low peak of droplet velocity (at around 66 ft/s) appeared at different times from y = 0.02 in (0.5 mm) to 0.16 in (4 mm) consistently signifying the occurrence of the droplet size variation due to secondary atomization of larger droplets from y = 0.02 in (0.5 mm) to 0.24 in (6 mm). At y = 0.24 in, occasional low peaks signified the occasional appearance of relatively larger droplets with lower velocity. In contrast, the timely consistency of droplet velocity of the SB spray at around y = 0.08 in again indicated the early completion of atomization. The droplets velocity increased from axial location of y = 0.02 in to 0.24 in for both FB and SB injectors. However, droplets velocity from SB sprays increased slightly from axial location 0.08 in to 0.16 in and kept at almost the same at y = 0.16 in and 0.24 in. This result consistently signified that secondary atomization by Rayleigh-Taylor instabilities was almost complete at y = 0.08 in for the SB injector with exit diameter of 0.06 in (1.5 mm), i.e. about 1.3 D downstream of the injector orifice.

Figure 28 illustrates time analysis of droplets axial velocity of FB and SB injectors at the periphery spray (x = 0.04 in), where most of larger droplets are observed from the primary atomization by bubble bursting *[7, 8]*. Larger droplets at periphery region move slower than finer droplets at the spray center. In Figures 28(a-b), the droplet velocity at the FB spray periphery increase from around 262 ft/s (80 m/s) to 459 ft/s (140 m/s) at y = 0.08 in (2 mm) to 0.24 in (6 mm). In Figures 28 (e-f), the velocity of around 262 ft/s (80m/s) for most droplets at SB spray edge changes slightly along the axial locations starting from y = 0.08 in (2 mm). Consistently, this indicates that the second atomization by SB swirling effect disintegrates most of larger droplets at periphery region into finer droplets by axial location of 0.08 in (2 mm).

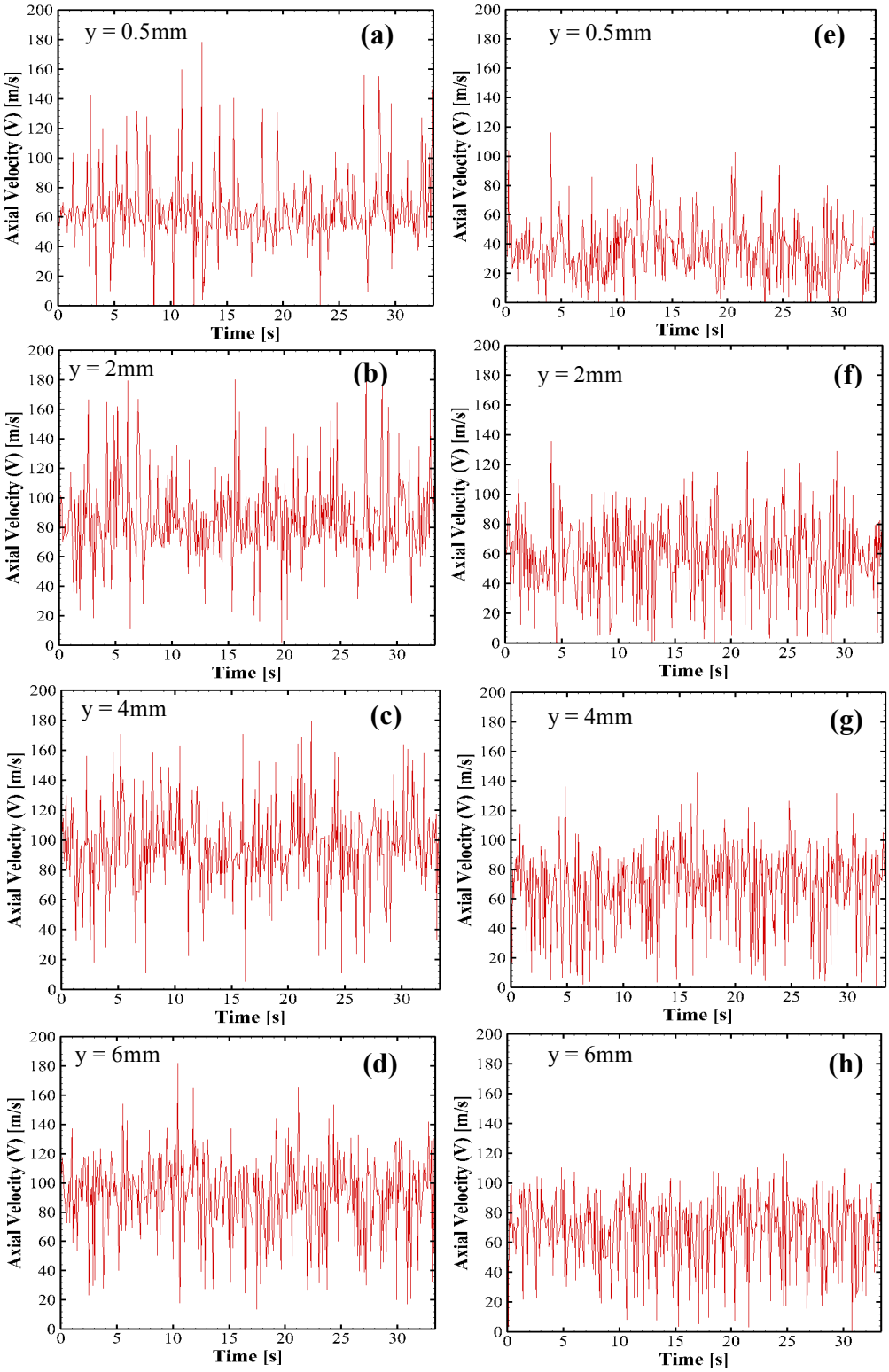

Figure 27

Time analysis of droplet axial velocity at x = 0mm for (a) – (d) FB injector, (e) – (h) SB injector.

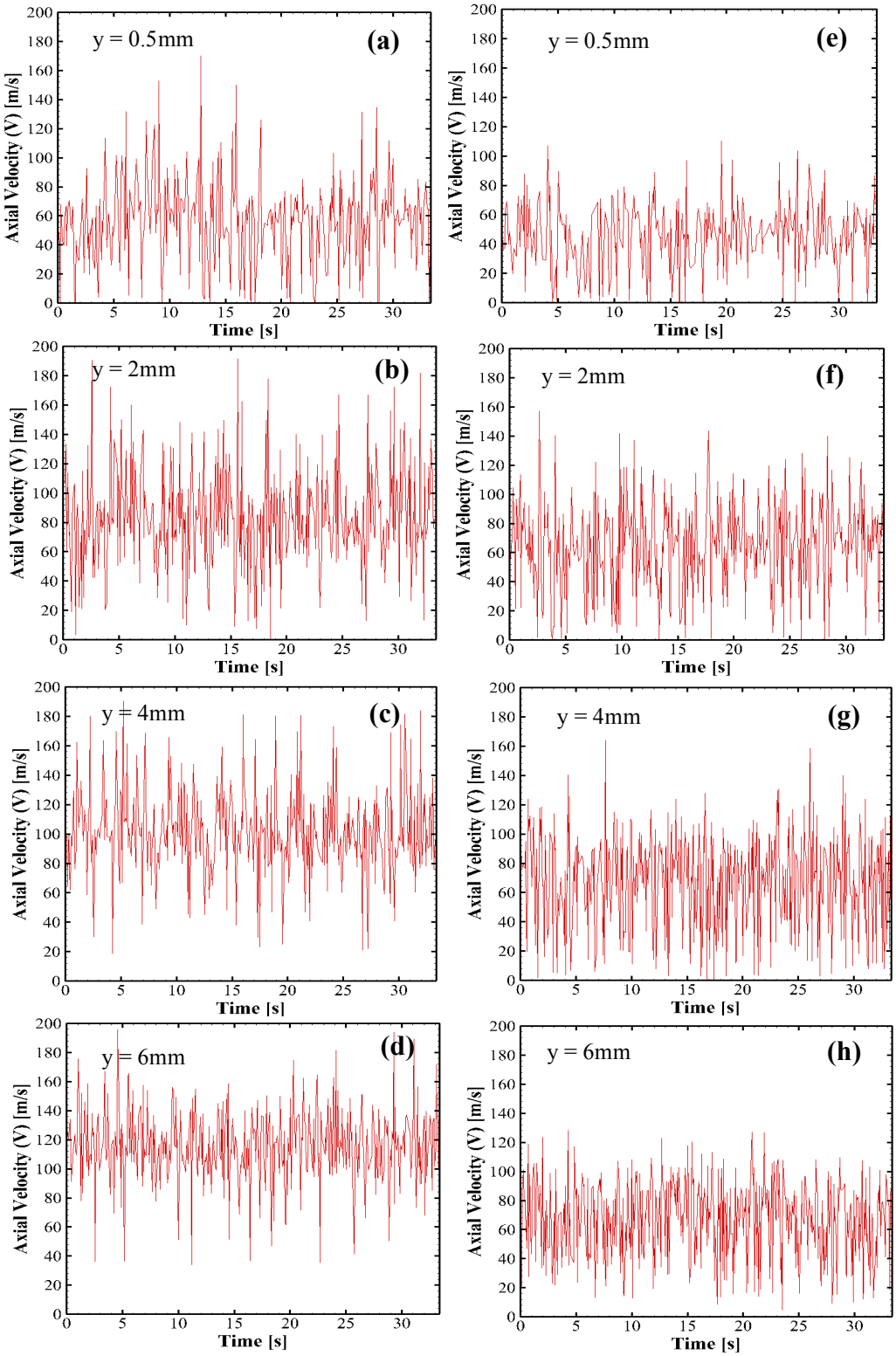

Figure 28

Time analysis of droplet axial velocity at x = 1 mm for (a) – (d) FB injector, (e) – (h) SB injector.

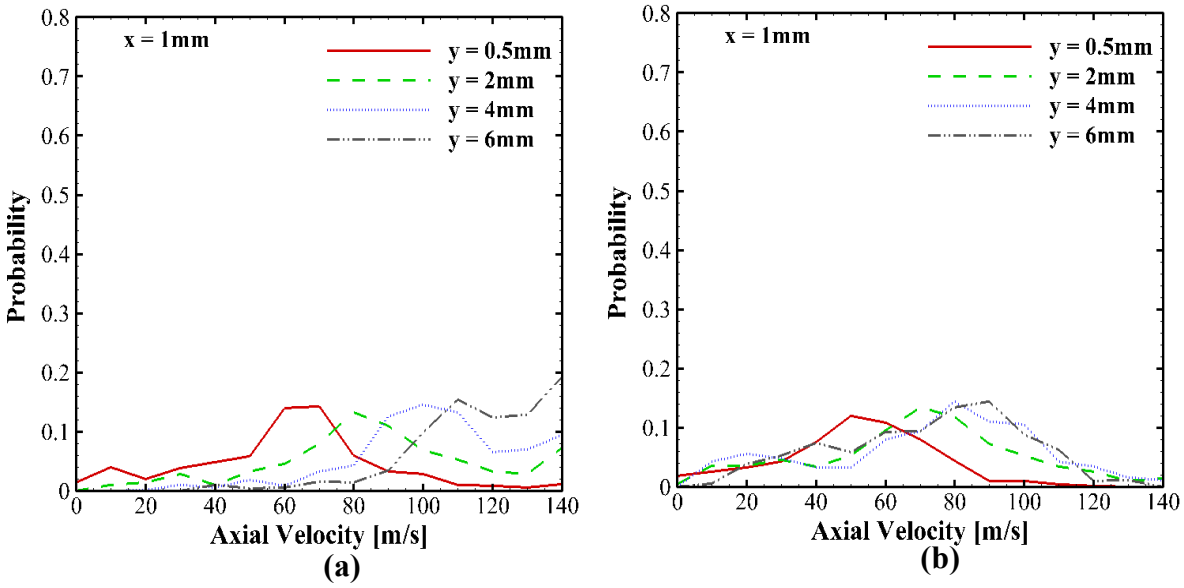

Figure 29

Probability distribution plots of droplet radial velocity at the center spray at different axial locations for: (a) FB injector, (b) SB injector

Figure 29 depicts the probability profile of droplet axial velocity at the spray periphery (x = 0.04 in) for FB and SB injectors from 500 consecutive measurements at different axial locations. The peak of the probability profiles of axial velocity indicated the velocity of most of the droplets at the tested locations. As shown in Figure 29(a), the majority of the FB droplets are traveling at around 213 ft/s (65 m/s) at y = 0.02 in (0.5 mm), which increased gradually to around 377 ft/s (115 m/s) with the increment of approximate 66 ft/s (20 m/s) for each axial location from y = 0.02 in (0.5 mm) till 0.24 in (6 mm) downstream of the injector orifice. In contrast, the slight shift in the peak droplet velocity from y = 0.08 in (2 mm) to 0.24 in (6 mm) of the SB spray coherently indicated the effective secondary atomization of larger droplets at spray edge accomplished at around 0.08 in (2 mm) downstream of the SB injector exit.

Pressure drop in AA lines across injectors is measured to compare energy input of the novel FB and SB injectors with a conventional AB injector which is effective for low-viscosity fuels but with limited atomization capability of heavy and viscous fuels. Figure 30 shows pressure drop in AA line across the injector increases with the increasing ALR because of the varying air flow rate and constant liquid flow rate. Pressure drop in AA line of the two novel injectors is apparently lower than that of the conventional AB injector, signifying less energy input for the two novel fuel atomizers with superior atomization capability. Pressure drop in

AA across FB and SB injectors are almost the same for all ALRs. Pressure drop in AA line is almost 2 psi at ALR of 1 and increasing to around 9 psi at ALR of 2.5 for both FB and SB injectors. This result indicates that SB injectors improve the secondary atomization by the SAA without requiring extra energy input. In summary, the SB injector further enhances the atomization capability for heavy and viscous fuels with much lower energy input required compared to a typical AB injector, potentially enabling more compact clean engines of heavy fuels with higher power to weight ratio.

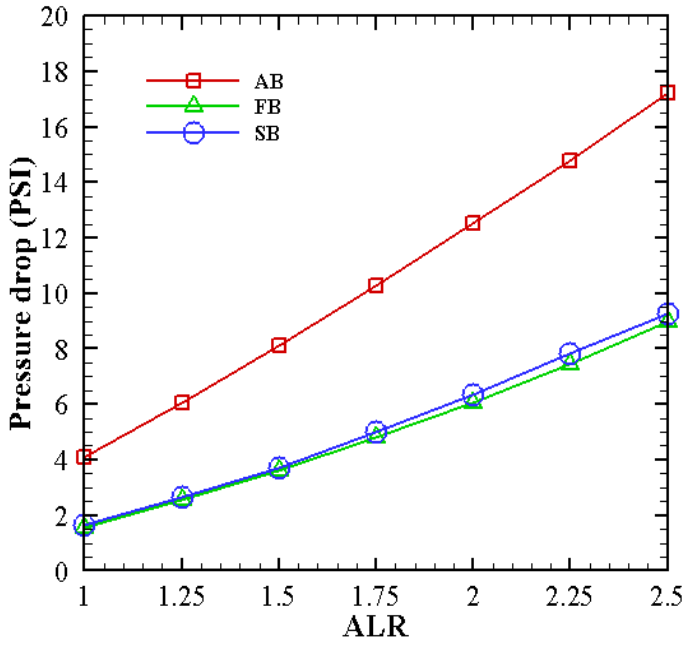

Figure 30
Pressure drop of atomizing air line across injectors

CONCLUSIONS

In this study, a novel swirl burst (SB) injector has been successfully designed by incorporating a swirling atomizing air with the flow blurring concept. The present project investigates combustion performance of the novel SB injector for various heavy and viscous fuels including vegetable oil (VO, soybean oil) and algae oil, which are source oils of biodiesel. This work also studies effect of ALR and the SB injector geometry in terms of swirl number on the combustion performance to gain insight into the optimum working flow rate range and effective geometry. Compared to FB injection, spray characterization in the near injector of a SB injector using PIV laser diagnostics further reveals the SB atomization mechanism with the introduced swirling atomizing air (SAA) effect. Comparison of the pressure drop in the AA line across the novel SB and FB injectors with that of a conventional AB injector shows the energy input required for the novel injection methods. Results of the present study are shown as below:

- Clean and complete lean premixed combustion of viscous VO and AO has been achieved using the novel SB and FB injectors without fuel pre-heating, saving the cost and energy of converting the source oils into biodiesel for conventional engines running on low viscosity fuels.
- Compared to FB injection, SB injector results in enhanced secondary atomization by the SAA and thus faster fuel evaporation as well as the less lifted flame, improving the flame sustainability and stability.
- The shorter pre-vaporization zone and compact flame obtained with the SB injector signifies improved fuel-air mixing, quicker fuel evaporation and faster fuel oxidation, yielding higher local reaction zone temperature.
- The low CO and NOx emissions obtained from the SB injector were slightly higher than those from the FB injector which is consistent with the higher local temperature obtained in the SB injector.
- Increase in ALR on SB injector further lowers the emissions due to finer droplets evolution.
- The less lifted flames and compact flame were however still retained at higher ALRs showing consistent improved fuel-air mixing, quick fuel evaporation and faster oxidation of fuel.
- The symmetry of the product gas temperature profile was consistent signifying uniform fuel air mixture and even droplet size distribution was achieved with the SB injector due to the swirling atomizing air.

- Nearly zero CO emissions and ultra-low NOx emissions (<10 ppm) of straight algae oil combustion have been achieved using the superior SB atomization for three swirl numbers (SNs) of 1.5, 2.0, and 2.4.
- SN of 2.0 of the SB injector yields the minimum NOx because of the enhanced atomization and appropriate axial velocity to sustain a less lifted flame with lower reaction zone temperature and thus minimize the thermal NOx formation.
- PIV spray images indicate fine droplets generated immediately at the SB injector exit, rather than a typical jet of conventional injectors, indicating its superior atomization capability.
- Quantitative PIV results including average spray velocity field, temporal analysis and probability of the droplet axial velocity for 500 consecutive image pairs consistently reveal that atomization completed at 0.08 inch (2 mm) downstream of the injector exit, which is about half of that of the prior-proved fine FB injection, indicating the further enhanced secondary atomization by the SAA.
- Pressure drop in AA line of the two novel injectors is apparently lower than that of the conventional AB injector, signifying less energy input for the two novel fuel atomizers with superior atomization capability.
- Pressure drop in AA across FB and SB injectors are almost the same for all ALRs, indicating that SB injectors improve the secondary atomization by the SAA without requiring extra energy input.

In summary, the present project successfully designed and tested a novel SB injector. Enhanced atomization by the novel injection resulted in less lifted flames and thus better flame stability. Ultra-low emissions for highly viscous and heavy oils including VO and AO have been achieved without fuel pre-processing indicating the extraordinary atomization capability and fuel flexibility. Low pressure drop across the SB injector signifies promise of more compact clean engines of heavy fuels with higher power to weight ratio.

RECOMMENDATIONS

According to the research results, the recommended future work includes:

- Investigation of spray size distribution to better understand the spray features and the propagation of flame structure.
- Investigation of internal flow visualization of the injector to fully understand the atomization mechanism for future practical applications.
- Understanding of the spray evaporation and dynamics to establish the correlation between spray physics and combustion dynamics for future high-fidelity modeling.
- Understanding of the combustion performance of various fuels and spray characteristics at engine simulated conditions, i.e., elevated pressures and temperatures to gain insight of the promise in real combustion systems.

ACRONYMS, ABBREVIATIONS, AND SYMBOLS

AA	Atomizing Air
AB	Air Blast
ALR	Atomizing-air to Liquid Mass Ratio
AO	Algae Oil
cm.	centimeter(s)
CO	Carbon monoxide
CO_2	Carbon dioxide
D	Diameter of liquid tube
d_h	Hub diameter
d_t	Tip diameter of swirl
F	Fahrenheit
FB	Flow Blurring
FOV	Field of view
fps	Frames per second
ft/s	Feet per second
H	Gap between liquid tube and injector orifice
HRR	Heat Release Rate
Hz	Hertz
in.	inch(es)
kW	kilo-Watt(s)
lab	Laboratory

lpm	Liters Per Minute
LPM	Lean premixed combustion
ml/min	Milliliter per minute
mm	millimeter(s)
NG	Natural Gas
No.	Number
NOx	Nitric oxide
PIV	Particle Image Velocimetry
ppm	Parts per million
psi	Pound per square inch
SAA	Swirling Atomizing Air
SB	Swirl Burst
slpm	Standard liter per minute
SN	Swirl Number
tan	Tangent
VO	Vegetable Oil
μm	Micrometer
α	Vane angle of swirl
≤	Less than or equal to
±	Plus or minus
^{o}	Degree

REFERENCES

1. Gañán-Calvo, A. M. "Enhanced liquid atomization: From flow-focusing to flow-blurring", *Applied Physic Letter*, Vol. 86, No. 21, 2005, pp. 2141-2142.
2. Panchasara, H., Sequera, D., Schreiber, W., Agrawal, A. K. "Emission reductions in diesel and kerosene flames using a novel fuel injector", Journal of Propulsion and Power, Vol. 25, No. 4, 2009, pp. 984-986.
3. Simmons, B. M and Agrawal, A. K. "Flow Blurring Atomization for Low-Emission Combustion of Liquid Biofuels", Combustion and Science Technology, Vol. 184, No. 5, 2012, pp. 660-675.
4. Simmons, B. M., Kolhe, P. S., Taylor, R. P., and Agrawal, A. K. "Glycerol Combustion using Flow-Blurring Atomization", The 2010 Technical Meeting of the Central States Section of the Combustion Institute (2010) Champaign, Illinois.
5. Jiang, L., Agrawal, A. K., Taylor, R. P. "Clean combustion of different liquid fuels using a novel injector", Experimental Thermal and Fluid Science, Vol. 57, 2014, pp. 275–284.
6. Jiang, L., Agrawal, A. K. "Combustion of straight glycerol with/without methane using a fuel-flexible, low-emissions burner". Fuel Vol. 136, No. 15, 2014, pp. 177–184.
7. Jiang, L., Agrawal, A. K. "Spray features in the near field of a flow-blurring injector investigated by high-speed visualization and time-resolved PIV", Experiments in Fluids, Vol. 56 No. 5, 2015, pp. 103.
8. Jiang, L., Agrawal, A. K. "Investigation of Glycerol Atomization in the Near-Field of a Flow Blurring Injector using Time-Resolved PIV and High-Speed Visualization", Flow Turbulence and Combustion, Vol. 94, No. 2, 2015, pp. 323-338.
9. Syred, N., Beer, J. M., "Combustion in swirling flows: A review", Combustion and Flame Vol. 23, No. 2, 1974, pp. 143–201.
10. Huang, Y., Yang, V. "Effect of swirl on combustion dynamics in a lean premixed swirl-stabilized combustor", Proceedings of the Combustion Institute, Vol. 30, No. 2, 2005, pp. 1775-1782.
11. Lilley, D. G. "Swirl Flows in Combustion: A Review", AIAA Journal, Vol. 15, No. 8, 1977, pp. 1063-1078.
12. Khandelwal, B., Lili, D., Sethi, V. "Design and study on performance of axial swirler for annular combustor by changing different design parameters", Journal of the Energy Institute Vol. 87, No. 4, 2014, pp. 372–382.
13. Department of Biological Sciences and Biotechnology, Tsinghua University, Beijing, China (2004) http://www.oilgae.com/algae/oil/oil.html

14. Mati, K., Ristori, A., Gaïl, S., Pengloan, G., Dagaut, P. “The oxidation of a diesel fuel at 1–10 atm: experimental study in a JSR and detailed chemical kinetic modelling”, Proceeding of the Combustion Institute, Vol. 31, No. 2, 2007, pp. 2939-2646.
15. Panchasara, H., Sequera, D., Schreiber, W., Agrawal, A. K. “Emission reductions in diesel and kerosene flames using a novel fuel injector”, Journal of Propulsion and Power, Vol. 25, No. 4, 2009, pp. 984-986.
16. Schwab, A.W., Dykstra, G.J., Selke, E., Sorenson, S.C., Pryde, E.H., “Diesel fuel from thermal decomposition of soybean oil”, Journal of the American Oil Chemist’s Society. Vol. 65, No. 11, 1988, pp. 1781–1786.
17. Keane, R.D., and Adrian, R.J. “Theory of cross-correlation analysis of PIV images”, Applied Scientific Research. Vol. 49, 1992, pp. 191 – 215.

APPENDIX

N/A